Bioactive Supramolecular Coatings with Macroscopic Alignment

Bachelor's Thesis

for obtaining the academic degree
Bachelor of Science
in the department of Chemistry, Pharmacy and Geoscience
of the Johannes-Gutenberg University

submitted by
Sabrina Helena Schmied
born September 26, 1996
in Princeton, New Jersey (USA)

Die vorliegende Arbeit wurde zwischen November 2018 bis Februar 2019 am Max-Planck-Institut für Polymerforschung in Mainz in der Arbeitsgruppe von Frau Prof. Dr. Tanja Weil unter der Betreuung von Dr. Christopher V. Synatschke angefertigt.

The work presented in this thesis was performed in the time between November 2018 until February 2019 in the group of Prof. Dr. Tanja Weil under the supervision of Dr. Christopher Synatschke at the Max Planck Institute for Polymer Research in Mainz, Germany.

Betreuer:	**Dr. Christopher Synatschke**
Erstkorrektor:	**Prof. Dr. Tanja Weil**
Zweitkorrektor:	**Prof. Dr. Pol Besenius**

Bachelorarbeit im Studiengang Chemie, Biomedizinische Chemie oder Polymerchemie an der Johannes Gutenberg - Universität Mainz

Ich, Sabrina Helena Schmied, Matrikelnummer 2725862 versichere, dass ich meine Bachelorarbeit selbstständig verfasst und keine anderen als die angegebenen schriftlichen und elektronischen Quellen sowie andere Hilfsmittel benutzt habe. Alle Ausführungen, die anderen Schriften wörtlich oder sinngemäß entnommen wurden, habe ich kenntlich gemacht.

_____   _____
(Ort, Datum)   (Unterschrift)

First of all, I want to thank Prof. Dr. Tanja Weil for giving me the opportunity to be part of her great work group - I really enjoyed my time at the MPIP.
Another big thanks to Christopher Synatschke, my supervisor, for including me into his team. I will always remember you as the pink fairy you truly are.
Also, thanks to Michaela Pieszka for being like a second supervisor for me.

Most important of all: thanks to my family, for always supporting me! Special thanks to my father, for being the person inspiring me the most.

Abstract

Inspired by biological tissues and their distinct microstructures, the interest of polymer chemistry and medicine in bioactive, anisotropic materials has grown throughout the past years. Considerably affected by this development is the research area of hydrogels as they displayed great potential for medical applications, especially in regenerative medicine, even without further alignment of their structural motifs.

In case a hydrogel comprises anisotropic properties, an additional improvement in qualities takes place: due to its spatial arrangement it becomes an "information carrier", improving the field of 3D cell cultures. Anisotropic hydrogels consisting of components of inherent biological origin, such as self-assembling peptides, would be a great asset for this field.

In this work, the peptide with the sequence CEFEFEF was synthesized, which derives from a peptide sequence that improved neuronal outgrowth *in vitro*.

The self-assembly of the prepared sequence was achieved and characterized and the results showed, that the highest quantity of fibers was documented at the peptide's isoelectric point. Furthermore, a hydrogelation of the fibers was realized with calcium chloride, and three different methods for aligning the high aspect ratio peptide nanofibers within this hydrogel were tested: a manual and an automated exposure to shear forces as well as the technique called zone casting. Hereby the most promising results were achieved by means of the automated shear force application.

The present thesis was inspired by the work of Stupp *et al.*, who was able to fabricate anisotropic hydrogels from peptide amphiphiles. Successful approaches would result in hierarchically ordered materials with macroscopic orientation of nanostructured building blocks. These structures would likely lead to novel properties, particularly in directing cellular growth and migration.

Zusammenfassung

Biologisches Gewebe hat durch seine ausgeprägten, streng orientierten Mikrostrukturen das Interesse für anisotrope Materialien in der Polymerchemie als auch der Medizin geweckt.

Insbesondere ist hiervon das Forschungsgebiet der Hydrogele betroffen, da diese bereits ohne Ausrichtung ihrer Wirkkomponenten einen hohen Stellenwert im Bereich der regenerativen Medizin einnehmen. Wird einem Hydrogel zusätzlich zu seinen Qualitäten, die es bereits seit einiger Zeit für medizinische Anwendungen qualifizieren, noch eine definierte räumliche Anordnung zuteil, so gewinnt es die Eigenschaft einer Art ”Informationsmedium” agieren zu können. Diese Eigenschaft steigert das Potential des Hydrogels für biologische Anwendungen wie z.B. extrazelluläre Matrix Immitate.

Zusätzlich werden die biologische Anwendbarkeit und Komplexität solcher Systeme gesteigert, wenn dessen Wirkkomponenten inhärent biologischen Ursprungs sind, wie beispielsweise selbstassemblierende Peptide.

Aus diesem Grund wurde in der vorliegenden Arbeit das Peptid CEFEFEF synthetisiert, das sich aus dem bereits bekannten, biologisch aktiven Peptid CKFKFQF ableitet.

Das Selbstassemblierungsverhalten des, in dieser Arbeit dargestellten Peptids wurde untersucht und charakterisiert, wobei festgestellt werden konnte, dass die ausgeprägteste Fibrillenbildung um den isoelektrischen Punkt des Peptides zu verzeichnen war. Darüber hinaus wurde mit Calciumchlorid ein geeigneter Induktor für die Hydrogel Bildung der Peptidfibrillen identifiziert, welches ein geeignetes Medium für die Fixierung der ausgerichteten Peptidfibrillen darstellt.

Für die beabsichtige Ausrichtung der erzeugten Peptidfibrillen wurden 3 Methoden getestet: die manuelle als auch die automatisierte Ausrichtung über die Einwirkung von Scherkräften und die recht neue Methode des Zone Castings, wobei die automatisierte Ausrichtung die vielversprechendsten Ergebnisse erzielte.

Die erfolgreiche Realisierung von bioaktiven Materialien mit makroskopischer Ausrichtung ihrer Nanostrukturen wäre eine Bereicherung für biomedizinische Anwendungen, da diese Materialien beispielsweise das Dirigieren von Zellwachstum- und Migration bewerkstelligen könnten.

Die vorliegende Bachelorarbeit wurde von den Arbeiten von Stupp *et al.* inspiriert, dem es bereits möglich war Peptidamphiphile in Hydrogelen auszurichten.

List of Abbreviations

ACN	Acetonitrile
AFM	Atomic force microscopy
Boc	Tert-butyloxycarbonyl
cryoEM	Cryogenic electron microscopy
DBU	1,8-Diazabicyclo[5.4.0]undec-7-ene
DIPEA	Diisopropylethylamine
DLVO	Derjaguin-Landau-Verwey-Overbeek Theory
DMF	Dimethylformamide
DMSO	Dimethyl sulfoxide
DOPA	3,4-Dihydroxyphenylalanine
ECM	Extracellular matrix
ESI-MS	Electrospray ionization mass spectrometry
eq.	equivalents
Fmoc	Fluorenylmethyloxycarbonyl
HPLC	High-performance liquid chromatography
LC-MS	Liquid chromatography–mass spectrometry
PBS	Phosphate-buffered saline
PyBOB	Benzotriazol-1-yl-oxytripyrrolidinophosphonium hexafluorophosphate
RT	Room temperature
SAP	Self-assembling peptide
SAXS	Small-angle X-ray scattering
SEM	Scanning electron microscopy
SPPS	Solid-phase peptide synthesis
TEM	Transmission electron microscopy
TFA	Trifluoroacetic acid
TIPS	Triisopropylsilane
TMS	Trimethylsilyl
UHMWPE	Ultra-high-molcular-weight polyethylene

Contents

1 Introduction

Current aspirations concerning biotechnology and in particular regenerative medicine, are targeting for artificial materials inspired by nature. However, it should be taken into consideration, that many nature-derived materials are highly oriented, contributing to their efficient functionality. Among these, anisotropic structures can be seen as one of the greatest assets in living organisms inclusive the human body. This recognition originated and fostered the field of anisotropic hydrogels from self-assembling peptides.

In the following, the underlying principles of this particular research area are further explained and accentuated with recent research results in a bottom-up manner.

1.1 Anisotropic Systems

Anisotropy is defined as a heterogenous order on a microscale within a macroscopic system.[1] Such systems show direction-dependent properties influencing the materials features, such as thermal behavior, hardness, and electrical conductivity. As shown on the schematic illustration Figure 1.1, both arrows pass through the same number of particles. Even though the horizontal arrow has a much longer way, it also passes only through golden particles whilst the diagonal arrow passes particles of both colors. It is evident that this simplified system shows different characteristics depending on the direction of observation.[2] Since anisotropic systems are highly organized, they show low values of entropy which is why the formation of anisotropic supramolecular assemblies is a nonequilibrium process.[3] Due to the highly ordered structure and hierarchical assembly of nanocomposites,[4] anisotropy plays a crucial role in many biological systems such as skeletal-muscle tissue. Muscle contraction is a result of the dense anisotropic structure in which actin and myosin are arranged within the sarcomere (Figure 1.2b)[5] generating highly directional motion. Furthermore this alignment ensures a higher efficiency of motion sequences than the corresponding isotropic version would.
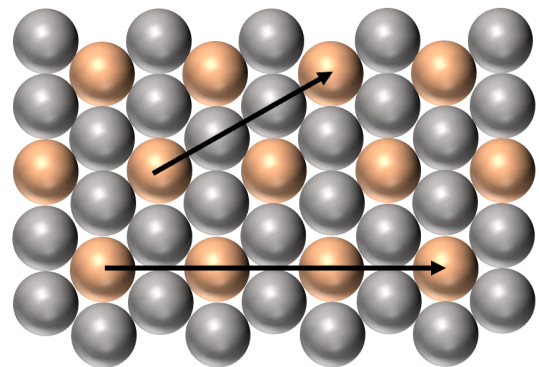

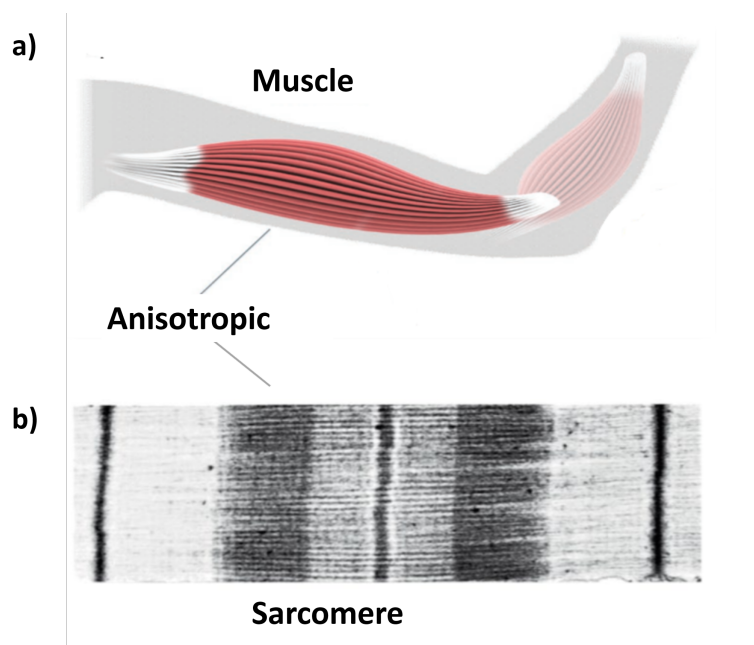Figure 1.1: Schematic illustration visualizing the concept of anisotropy.

Figure 1.2: Example for anisotropic alignment within the human body. **a** Schematic anisotropic orientation in muscle tissue.[4] **b** Electron micrograph of a myofibril from the skeletal muscle in longitudinal section, showing a single sarcomere.[6]

1.2 Self-Assembly

The process of self-assembly can be described as an autonomous and spontaneous formation of structures by already existing individual components, maintaining their preceding character upon integration into the supramolecular structure.[7], [8]

This assembly into supramolecular entities is based on attractive and repulsive chemical interactions involving electrostatics, van der Waals forces, π-π-stacking, hydrophobic effects, as well as coordinative- and even covalent bonds.[9]

The process of self-assembly is driven towards an equilibrium state.[8], [10] Due to the higher energy content of the unassembled components, as compared to the merged system, there is not only no additional energy input required, but the formation of a supramolecular structure is even leading to an overall energy minimization of the system.[8]

Even though self-assembly is defined as a process without further human contribution,[7] it is nonetheless possible to modify a molecule to such an extent, that it develops the characteristics of a self-assembling component. Such a modification would for example be the addition of a lipophilic hydrocarbon chain to a hydrophilic molecule for the purpose of mimicking the behavior of surfactants when self-assembling to micelles (Figure 1.3b). This particular behavior is driven by hydrophobic effects of the hydrocarbon chains as demonstrated by peptide amphiphiles (Figure 1.3a, c) in work by the group of S. Stupp.[11]
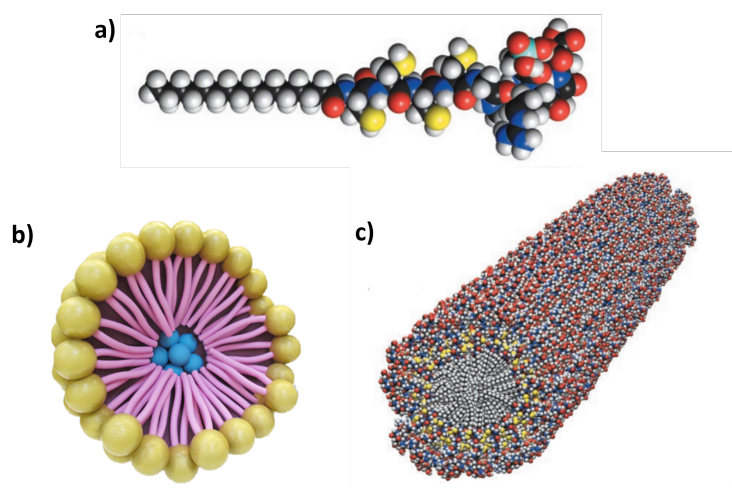
Figure 1.3: Self-assembling systems or compounds. **a** Peptide amphiphile,[11] **b** 3D scheme of a micelle,[12] and **c** cylindrical micellar structures from **a**.[11]

1.3 Hydrogels

Hydrogels are hydrophilic 3D polymer networks, capable of absorbing up to thousands of times their dry weight in water or biological fluids.[13],[14]
They constitute the most prominent research area in material science of our time and owe their popularity to their unique properties such as their high water content, flexibility and softness. These characteristics also make them one of the more promising candidates to mimic natural soft tissue for biomedical applications, such as drug delivery systems, encapsulation of cells or possibly even artificial muscle tissue.[14]

As hydrogels often lack mechanical stability, they have not yet demonstrated a sufficient ability to mimic muscle tissue, which could be an interesting example for functional anisotropic hydrogels. Hydrogels are typically composed of randomly oriented polymer networks, but more recent approaches deal with so called anisotropic wood hydrogels (Figure 1.4).[4]

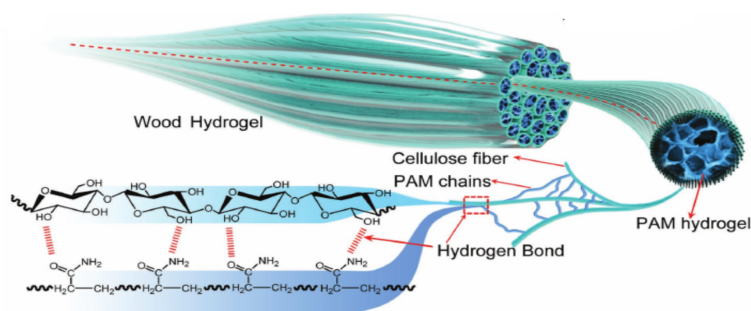

Figure 1.4: Depiction of the highly anisotropic wood hydrogel showing hydrogen bonding and covalent cross-linking with polyacrylamide chains.[4]

Hereby a muscle-like, ionically conductive, and highly anisotropic hydrogel is established by removing lignin from natural wood, which accounts for its rigidness, and replacing it with soft polyacrylamide Figure 1.4. Thus the wood's natural anisotropic cellulose-nanofibers are preserved and create a soft, yet aligned material without applying external forces. Also there is no need for further fixation as the polyacrylamide is inserted between already existing structures that act like a mold until the polyacrylamide is completely crosslinked with the cellulose.

Due to its proven sarcomere-like alignment (Figure 1.2b), biocompatibility, and greater stability, this opens a new field for nature-inspired anisotropic hydrogels, within the discipline of tissue-engineering.[4]

1.4 Self-Assembling Peptides (SAPs)

Since the coincidental discovery of SAPs by S. Zhang in 1990, this topic has grown to become one of the major biomedical research areas of the present times, supported by the relatively simple and affordable accessibility of peptide sequences.[15]

This development was facilitated by the Nobel Prize-winning invention of solid-phase peptide synthesis by R. Merrifield.[16] He revolutionized peptide synthesis as his concept allows to produce peptides with greater yields and within a very short time.[17]

As self-assembly counts to one of the biological indispensable principles of life, contributing to the formation of cells and membranes, it had to bear such a strong basis for new research approaches, especially regarding peptide nanobiotechnology and regenerative medicine.[15]

As peptides and their building blocks are naturally occurring constituents of the body and the extracellular matrix (ECM), which is showing a filamentous architecture, fibrillar hydrogels from self-assembled peptides derivingly show great abilities to mimic the ECM and therefore qualify for 3D cell cultures.[18] Experiments suggested that SAPs serve as wound dressings as they enable reephitalization by covering the surface of the wound.[19]

If the peptides within the hydrogel contain specific bioactive amino acid motifs, the hydrogel improved axon regeneration. In an experiment with mice suffering from spinal cord injury, peptide amphiphiles succeeded in inhibiting glial scar formation. For this purpose, a liquid containing fibers from peptide amphiphiles was injected directly into the spinal cord where further self-assembly-behavior was triggered by the *in vivo* environment.[20]

Further promising results could have been achieved by not only utilising the bioactive nature of the peptide, but also by tapping into physical information, such as spatial arrangement. The importance of spatial arrangement can be derived from the precision of neuronal connections which is required during the neuronal migration of postmitotic neuroblasts in the fetal brain. Hereby the migrating neurons are guided to their destination by attaching themselves to highly oriented radial glia cells.[22]

This highly oriented network of radial glia is essential for the complex development of the brain, showcasing that anisotropic structures are necessary to successfully mimic human tissue.

1.5 Origin of the Peptide Sequence

In the course of establishing a peptide library, S. Sieste identified the self-assembling peptide CKFKFQF.[23] This sequence showed improved neuronal outgrowth as well as enhanced transduction of viruses in vitro.[24] The structure of this sequence comprises three features that have proven to be of significance for the self-assembling process. First of all the polar side chains of the peptide stabilize the self-assembled structures in aqueous solution, by imitating the behavior of micelles (Figure 1.3b). Secondly, it follows the pattern of alternating hydrophobic and hydrophilic amino acids which have proven to be beneficial for the process of self-assembly, as such peptides show a tendency to adopt β-sheet structures.[25]–[27] Hereby the side chains segregate to opposing sides of the peptide backbone. All hydrophilic amino acids (lysine, glutamine) are located on one side, forming complementary ionic bonds, whereas all hydrophobic amino acids (phenylalanine) are located on the other side, performing π-π-interactions. That way the structure of a facial peptide is developed which can congregate into "sandwich-structures".[21] Another feature is introduced by the integration of cysteine into the peptide sequence. Omitting this amino acid results in the sequence KFKFQF, which showed diminished ability to self-assemble.[23] This could indicate that the presence of cysteine is necessary for the formation of β-sheet-like structures. Stupp *et al.* postulated that cysteine increased the robustness of nanotubes made of peptide amphiphiles by covalent capture of the supramolecular fibers. They argued that cysteine is able to form covalent disulphide bridges by oxidation, which also contributes to the tertiary structure in proteins.[11]

Even though the peptide showed good ability for fiber formation, it only showed weak ability in forming hydrogels. Therefore, the acidic counterpart CEFEFEF was designed for this bachelor's thesis, exchanging the amino acids lysine and glutamine for glutamate. As a consequence of this sequence modification, the biological activity of the original sequence[24] should be preserved while fostering the peptide's ability to form hydrogels.
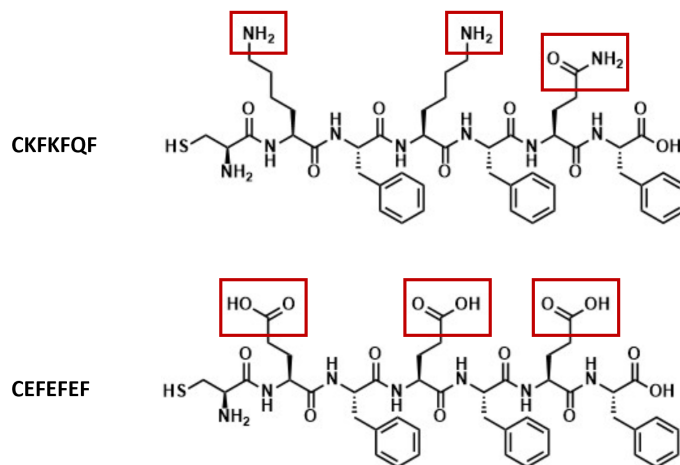

Figure 1.5: Structural formulas of the peptides CKFKFQF and CEFEFEF. Red boxes emphasize the difference of the functional groups within the side chains.

1.6 Alignment Methods

Inspired by naturally appearing anisotropic systems, such as aligned collagen fibers within the stroma cornea of the eye,[28] various techniques to recreate such structures were established within current research, for example by means of a magnetic- or electric field or through the impact of shear forces.

These ambitions are based on the change of features upon alignment of the the materials compounds. Through the alignment of the collagen fibers for example, the stroma cornea exhibits a transparency which is essential for vision, in contrast to the unaligned fibers.[29] Knowledge of this kind led to the discipline of creating highly oriented polymers as well as hydrogels

An example for a common, highly oriented polymer is ultra-high-molecular-weight polyethylene (UHMWPE), marketed under the name Dyneema by DSM. The alignment of the super drawn fibers is achieved by means of a gel spinning process in which polymer fibers are stretched, spinned and thermally treated. The resulting extremely long and oriented fibers cause a high stability, tenacity, and modulus of the material based on the high number of van der Waal interactions, enabling the material to be applied in military ballistic-resistant vests.[30]

As hydrogels count to low invasive materials and therefore do not exhibit mechanical stability comparable to UHMWPEs, it is not possible to achieve an alignment by applying intense mechanical forces. Therefore, other methods to obtain alignment must be considered.

Aida *et al.* established an alignment of negatively charged titanium sheets within a thermoresponsive hydrogel by means of a magnetic field. Hereby an anisotropic hydrogel that was able to perform an earthworm-like peristaltic crawling was created. This showcases that a system upon alignment can imitate natural movement, showing potential for application in remotely controlled medical devices.[31]

De Laporte *et al.* established an 'Anisogel' upon aligning magneto-responsive fibers, in the direction of an external magnetic field. The aligned bioactive fibers exhibit the ability to support unidirectional nerve growth (Figure 1.6f),[32] comparable to radial glia mentioned in chapter 1.4.
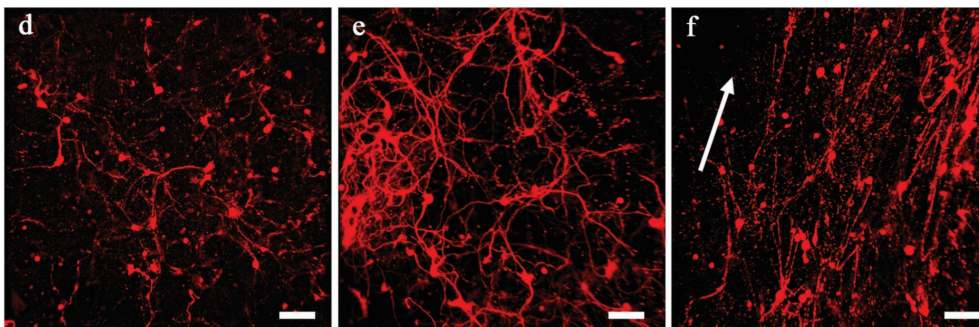

Figure 1.6: In red: neurite extensions of single neurons in a hydrogel showing **d** no fibers, **e** fibers without orientation, and **f** aligned fibers (inset arrow). Scale bars are 100 µm.[32]

Zhou *et al.* established a pathway of creating anisotropic hydrogels via enzymatic hydrogelation and π-π-interactions, enhancing fibrous alignment.[28]
Yet another group succeeded in growing aligned size-controlled self-assembled diphenylalanine peptide nanotubes on a polyether sulfone membrane.[33]

Another method to obtain alignment, which delivered great results in the last couple of years, was achieved by applying shear forces onto fibers.
Stupp *et al.* were able to create cellular wires by means of this method Figure 1.7. Hereby supramolecular filaments were mixed with cells and injected into a saline solution using a pipette (Figure 1.7a). This method did not require the impact of extensive shearforces, as the small nozzle created hydrogel strings containing highly oriented peptide amphiphiles[34] that allowed cells to grow along the aligned fibers (Figure 1.7b-d).
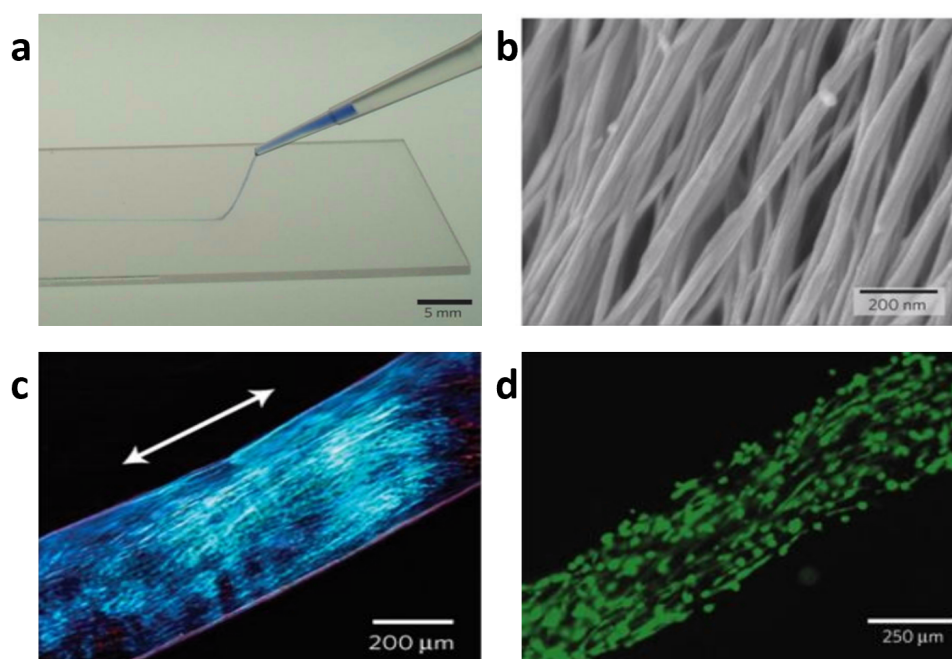
Figure 1.7: Anisotropic cellular wire from peptide amphiphile hydrogel. **a** Drawing the peptide amphiphile solution from a pipette into a calcium chloride solution, resulting in an instant hydrogelation. **b** SEM image of the aligned fibers within the hydrogel which is also showing **c** birefirngence under polarized light. **d** Calcein-labelled cells growing along the aligned fibers within the wire.[34]

Based on this strategy Hartgerink *et al.* established an anisotropic hydrogel from peptide fibers without a hydrocarbon sidechain but with incorporated DOPA. The achieved alignment was preserved by means of oxidizing the DOPA, leading to a covalent cross linkage of the fibers.[35]
Feringa *et al.* aligned self-assembled, photo responsive amphiphilic molecular motors, again by drawing a solution of those molecules into calcium chloride solution. This way an unidirectionally aligned string that is able to bend upon light exposure was fabricated (Figure 1.8).[36]
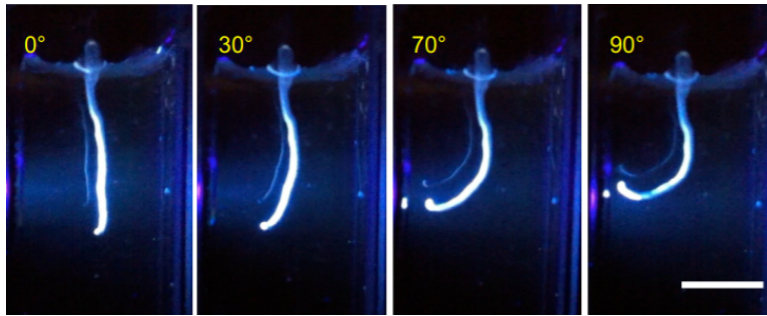
Figure 1.8: Actuation by means of UV light of the string from molecular motors in aqueous solution. The string is bending towards the light source. Scale bar is 0,5 cm.[36]

Within this discipline of aligning hydrogels, Stupp *et al.* managed yet another breakthrough: they created circumferentially aligned peptide amphiphile nanotubes(Figure 1.3c) and preserved the achieved alignment in the form of an anisotropic hydrogel by adding multivalent calcium ions[37], [38] .

This was realized by means of the construction shown in Figure 1.9.
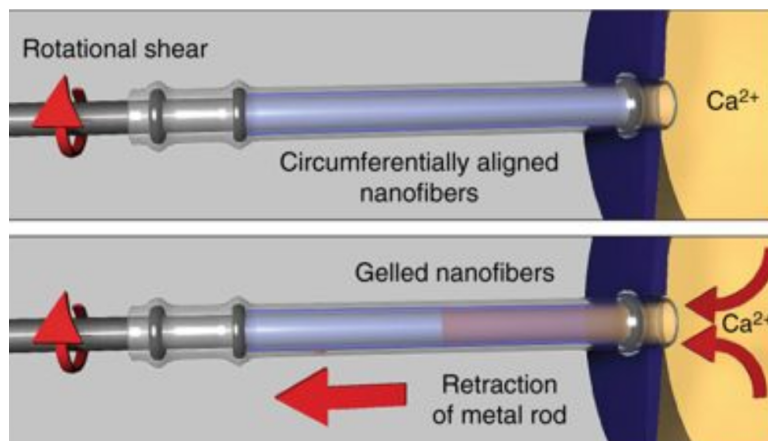
Figure 1.9: Construction to fabricate the hydrogel tubes. Circumferential shear forces are applied to a peptide solution to align the fibers. When removing the rod, a calcium chloride solution floods the vessel, resulting in an instant hydrogelation of the fibers.[38]

A simplified alteration of the construction Figure 1.9 to create linear hydrogels by means of either manual or automated shear force application was applied in the course of the present thesis, which will be introduced in chapter 3.4.1.

Another method, which is not using shear forces to induce alignment, is newly introduced to the process of aligning fibers. This technique is referred to as zone casting. It offers a way to create anisotropic coatings from macromolecular materials,[39] for example the active layers in photovoltaic cells.[40]
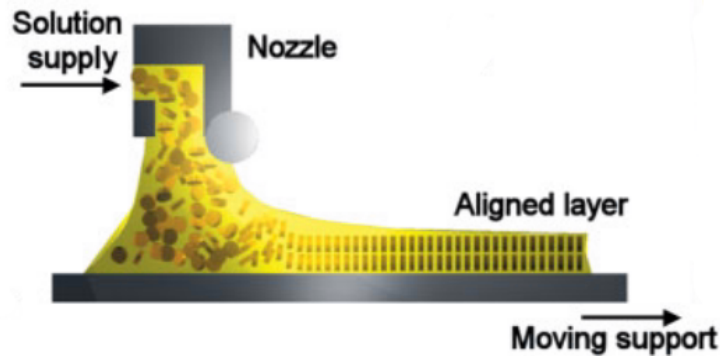
Figure 1.10: Schematic figure of the zone casting process.[39]

Hereby the substance is continuously supplied by a nozzle onto a moving microscope slide (Figure 1.10). Under appropriate amounts of solution supply and solvent evaporation, regulated by thermocontrol of the slide as well as the solution itself, a stable meniscus can be formed. This meniscus is providing a stationary gradient of concentration of the deposited material, resulting in a directional crystallization.[40]

The present thesis follows the idea of the introduced research results, aiming towards the establishment of an anisotropic SAP hydrogel qualifying for 3D cell cultures.

1.7 Methods to Detect Alignment

There are manifold methods how to detect achieved alignment.
The easiest accessible way to verify anisotropy is by means of polarized optical microscopy. Hereby, it is possible to detect anisotropic materials by means of polarized light as they exhibit birefringence. When an anisotropic material is placed under cross polarized light, it shows four extinction positions as well as so called interference colors, when rotated 360 degrees. Isotropic materials do not exhibit birefringence and therefore the material stays dark throughout the rotation siehe Figure 1.11b.
Three methods allow a closer look onto the structural conditions of the aligned sample. Scanning electron microscopy (SEM) enables to get a detailed impression on the surface topography of the upper layer of the sample. In contrast, polarized optical microscopy allows to detect alignment throughout all layers of a transparent sample. Atomic force microscopy (AFM) gives an ultra-high resolution image of the materials surface and is therefore comparable to SEM, even though measurements with this method require more time and only allow imaging small areas of the sample.
Transmission electron microscopy helps to elucidate the structure of the material's components and a possible alignment on the smallest scale. As grits do not exhibit great mechanical stability, alignment via shear forces can not be measured by means of this technique.

Furthermore, it only allows to analyze small areas of the sample, which is why it is unsuitable for a detection of a macroscopic alignment.

Another method to detect alignment is small-angle x-ray scattering (SAXS) which allows the analysis of the large-scale orientation of a sample. Scattering of aligned samples would show ellipsoidal patterns, whereas unoriented samples do not exhibit an angular dependence of the scattering. In order to measure SAXS of self-assembling peptide samples, typically, high energy X-rays from synchrotron facilities are necessary.[37], [38]
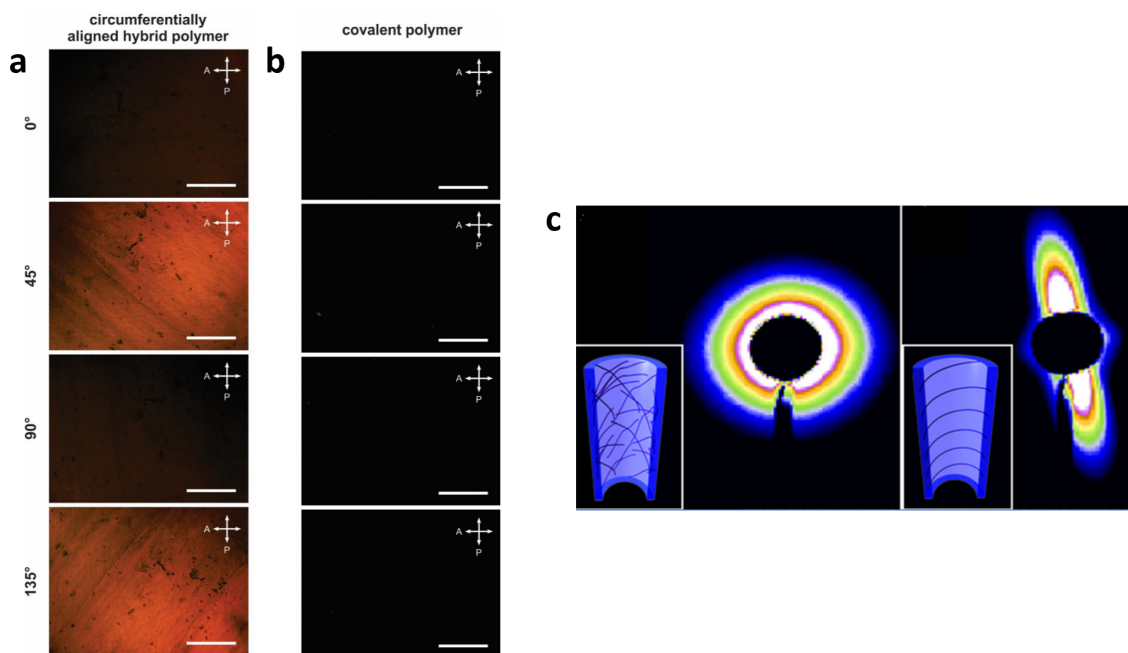
Figure 1.11: Analytical results from aligned systems. **a** and **b** Images from polarized optical microscopy under cross-polarized light. Scale bars at 400 μm **a** Exhibits birefringence while **b** showcasts that isotropic materials stay dark throughout the rotation of the sample by 0, 45, 90 and 135 degrees.[38] **c** Shows the resulst of an unaligned (l) versus an aligned (r) sample.[37]

In the present work, polarized optical microscopy was chosen to identify the overall alignment of the sample, SEM to enable a closer look at the sample's upper layer, and TEM to detect the self-assembly of the peptide into fibers.

2 Motivation and Objectives

The objectives of the present thesis are to identify the parameters for creating a SAP-hydrogel from the peptide sequence CEFEFEF and develop a method to establish anisotropic, homogeneous coatings using the hydrogels, which might qualify for highly oriented 3D cell cultures for neuronal cell growth.

Within the framework of this thesis, the bioactive self-assembling peptide CKFKFQF should be modified with the objective of fostering the peptide's ability to form hydrogels, while maintaining the bioactive properties as well as the ability to self-assemble into high aspect ratio peptide nanofibers. Therefore, the basic amino acids of the peptide should be exchanged by acidic ones, maintaining the alternation of hydrophobic and hydrophilic amino acids.[25]–[27] The negatively charged counterpart CEFEFEF should be prepared by means of SPPS, and purified via quantitative HPLC.
After preparing the peptide sequence, the conditions for triggering fibrillation should be characterized. Therefore, adjustment of parameters such as pH-value, counterions, and salt concentration should be examined.
Additionally, a fitting counterion for inducing hydrogelation of the prepared peptide should be identified, following up the work of Stupp *et al.*[38]

The identified parameters capable of forming SAP-hydrogels should be applied for creating coatings. Hereby not only an even, but also an anisotropic coating should be obtained by aligning the peptide fibers. For this purpose, different methods should be investigated: besides manual shear forces also automated shear forces should be applied by means of an electric film applicator. Other than that, the zone casting technique, performed in the group of P. Blom at the Max Planck Institute of Polymer Research, should be introduced to this new type of application.
The obtained alignment should be fixated within a hydrogel by adding the identified hydrogelation-triggering counterion.
The fabricated coatings should be examined for alignment by SEM and polarized optical microscopy.

3 Results and Discussion

The following chapter provides the results gathered throughout this work as well as their interpretation.

3.1 Peptide Synthesis

In the following section the results of the solid-phase peptide synthesis as well as the subsequent purification of the synthesized peptide are presented.

3.1.1 SPPS

For the required peptide with the sequence CEFEFEF the method of automated, microwave assisted SPPS was chosen, as it offered the easiest way of generating the highest yield within a short time. Therefore, the synthesis pathway for the sequence CKFKFQF by O. Ceyhun[23] was transferred to the synthesis of CEFEFEF by exchanging the respective amino acids. He described that a double coupling of the last amino acid, namely cysteine, dramatically improved the yield, which is why this step was also implemented.
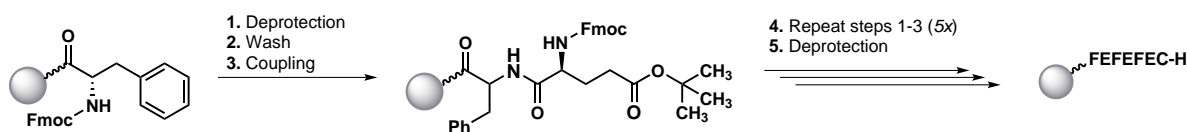
Figure 3.1: Simplified schematic illustration of the conducted SPPS.

Figure 3.1 shows a simplified scheme of the conducted SPPS, whereas a more detailed description can be found in chapter 5.2 of the experimental section.

For the synthesis the N-terminus of the resin linked amino acid, in this case phenylalanine, had to be deprotected by means of piperidine, whereas a second, still N-protected amino acid was activated by means of DIPEA/PyBOB. After the reaction of those two amino acids, the respective steps were repeated five times until the intended sequence was obtained. In between the repetitions the sequence had to be washed in order to minimize mismatches, showcasing yet another advantage of the SPPS, as the covalently linked peptide sequence could be washed over and over again, without losing significant amounts of product.

For future synthesis it should be taken into consideration to exchange piperidine for piperazine/DBU as it was proven to be more effective for deprotection, minimizing deletion sequences and racemisation, resulting in a yield optimization.[41]

3.1.2 Purification and Characterization

After completion and cleavage of the peptide from the resin, the peptide solution was purified via quantitative reversed phase HPLC. The peptide containing fraction was eluted after 10.61 min respectively at approximately 16% ACN. This can be explained by the relatively high polarity of the peptide due to its four hydrophilic amino acids.

Fractions containing the desired peptide were identified by means of ESI-MS measurements and lyophilized afterwards. A yield of 58.1% was obtained.

In order to verify whether the purification was successful, a LC-MS measurement was conducted.
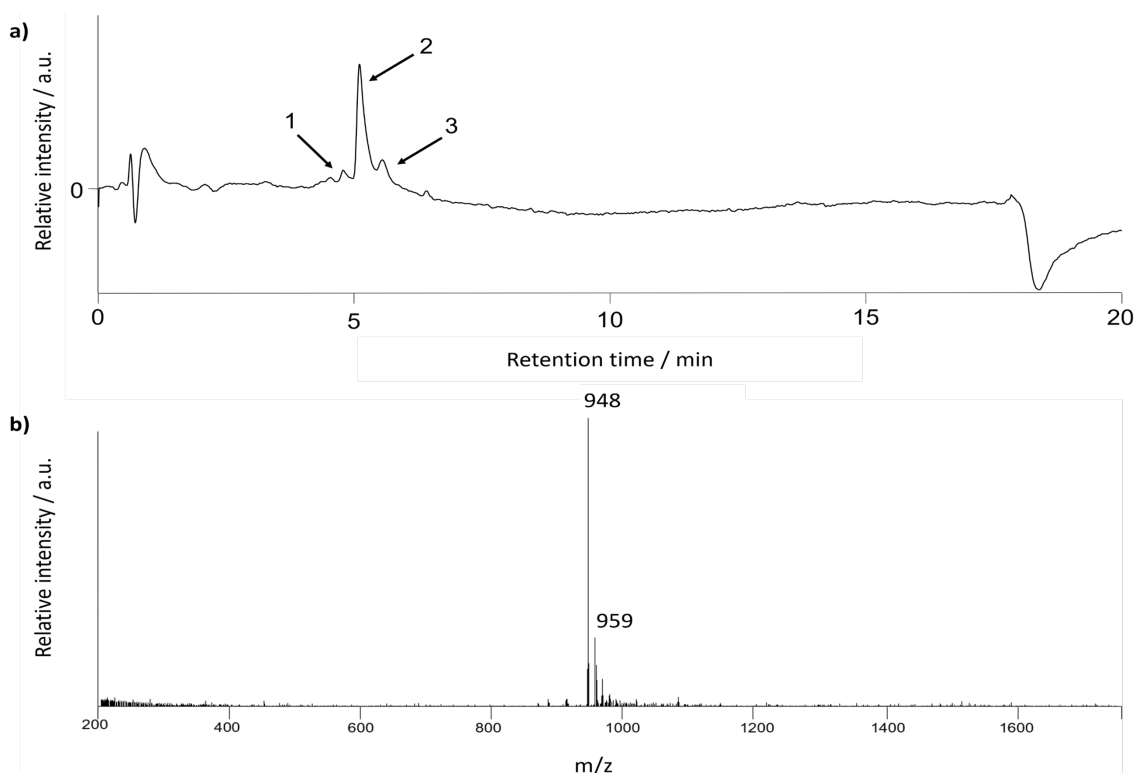
Figure 3.2: LC-MS spectra of the synthesized peptide **a** LC-trace with three labeled peaks. **b** Mass trace (-) with two labeled peaks, whereas the peak at 948 m/z belongs to [CEFEFEF]$^-$, the peak at 959 m/z belongs to an impurity.

The LC-trace in Figure 3.2a shows three peaks that appear after approximately 5 min retention time.

The corresponding mass trace in Figure 3.2b shows the highest peak at a m/z of 948 and

another one at 959.

The peak at 948 m/z corresponds to the expected mass of the intended peptide ([CEFEFEF]$^-$), proving that the synthesis was successful.

Furthermore, the peak at 959 m/z in the mass trace belongs to an impurity as the LC-trace also shows more than one peak of which two peaks, 1 and 3, are flanking the main peak 2, this underlines the presence of an impurity. As all three peaks have a similar retention time, this points to a chemical similarity of the detected substances. Also the m/z of the peptide's peak and the peak caused by the impurity, are very similar. This and the comparable chemical behavior suggest, that the impurity is probably caused by an erroneous sequence, at least partly composed of the same building blocks as CEFEFEF.

Analyzing the spectra by means of a computer software, the impurity is found in the first peak as well as the beginning of the main peak, while the mass of CEFEFEF is found in peak 2 and 3. This shows that the impurity is slightly more hydrophilic than the peptide.

Upon integration of the peaks, whereas peak 1 makes up 4,77%, peak 2 91,13% and peak 3 4,1%, this only enables stating that at least 4,77% of the yield are caused by the impurity.

Still the peptide shows a smearing behaviour as it does not appear in a sharp, single peak but two peaks and therefore exhibits the tendency of tailing. This could be due to many reasons such as solvent effects or strong interactions with the column. Another possible reason for this behavior could be caused by the TFA added to the mobile phase, which protonates the carboxylates of the peptide, potentially promoting its self-assembly behaviour. Therefore, peptide fibers or aggregates could have been formed in solution. This behaviour would most likely affect the interactions of the peptide with the column and therefore cause tailing.

To learn more details of the exact structure of the impurity, a peptide sequencing followed by mass spectrometry would have to be done. Furthermore, to achieve a better purification of the peptide, the ACN gradient, which was applied during HPLC (experimental section, chapter 9.4) would have to ramp up slower to allow a better separation. Other than that, the acidic mobile phase used for LC-MS measurements could be replaced by a basic solvent to prevent fiber- or agglomerate formation.

Since the impurity was probably caused by a peptide with similar chemical characteristics as the desired sequence, it was chosen to not perform further purification as the attempt would result in a dramatic loss in yield.

3.2 Initiation of Self-Assembly

Subsequently, the self-assembly behavior of the synthesized peptide in the presence of different salts and pH values was investigated. These parameters were chosen as they are known to critically influence self-assembly of small peptides.[36],[42] In order to maintain an alignable structure that allows the establishment of oriented supramolecular nanostructures, high aspect ratio peptide nanofibers should be obtained from the synthesized peptide sequence. By screening different self-assembly triggering conditions, the formation of long fibers should be

achieved, while simultaneously gaining a better understanding of the self-assembly behavior of the material.

As the peptide CEFEFEF contains three glutamic acids, capable of forming salts, suitable cations were required in order to maintain effective charge-screening ability, which could induce fiber formation according to the Derjaguin-Landau-Verwey-Overbeek (DLVO) theory. This theory offers a predicition on how to promote self-assembly, which can be transferred to the field of SAPs. It states that self-assembly should occur, when a system, even in absence of exogenous counterions, is electrically neutral to the outside, while still carrying charges.[42] Based on this theory, two parameters were varied in the course of screening for optimal self-assembly conditions: type of counterion and pH-value. Additionally, the incubation time was added as a third variable, as to potentially having an influence on the fiber forming process. Since the obtained fibers should eventually be applicable in the human body, either physiological or very low salt concentrations of the prepared solutions were used for the following experiments (Table 3.1).

Table 3.1: Overview of the applied solvents and their concentrations.

Solvent	Salt concentration
Milli-Q	-
Sodium chloride solution	$150\,\text{mM}$
Calcium chloride solution	$5\,\text{mM}$
Aluminium chloride solution	$100\,\text{mM}$

To screen a large number of different conditions triggering the self-assembly of the synthesized peptide and assess the resulting nanostructure would require excessive, time-consuming TEM measurements. Instead fluorescence assays were conducted. These are used to detect amyloid type aggregates, resulting in an increase in fluorescence. Elevated fluorescence intensity indicates the presence of fibrous aggregates. The thioflavin T assay was proven to be capable of allowing to draw conclusions from the relative fluorescence intensity to the quantity of fibers in the measured sample.[43] In this work the PROTEOSTAT® assay is used, which shows similar behavior as thioflavin T. Therefore, PROTEOSTAT® assays should also be capable of providing quantitative analysis of peptide aggregation.

For the implementation of the fluorescence assay, the fluorescence-causing agent was added to each solution and the mixture incubated for exactly $15\,\text{min}$ while shaking, to provide a homogeneous distribution of the active components. This procedure was repeated after $48\,\text{h}$ and $72\,\text{h}$.

In the following, the results of the applied counterions-, pH-, as well as incubation time variations, to induce the self-assembling behavior of the synthesized peptide, are presented.
Hereby 'high values' of fluorescence intensities are defined as those reaching levels higher than

40000, while 'no fluorescence' is defined as intensities up to 10000, since such low values can be detected in solutions without added peptide. Everything in between probably contains fibers but in such low quantities, that it would have been difficult to locate them on a TEM grid. Therefore only the samples exhibiting high intensities are further analyzed by means of TEM.

3.2.1 Solvent: Milli-Q water

Four peptide solutions in Milli-Q water within a range of pH 4 - 7 were prepared. After an incubation time of 24 h, 48 h, and 72 h fluorescence assays were conducted.
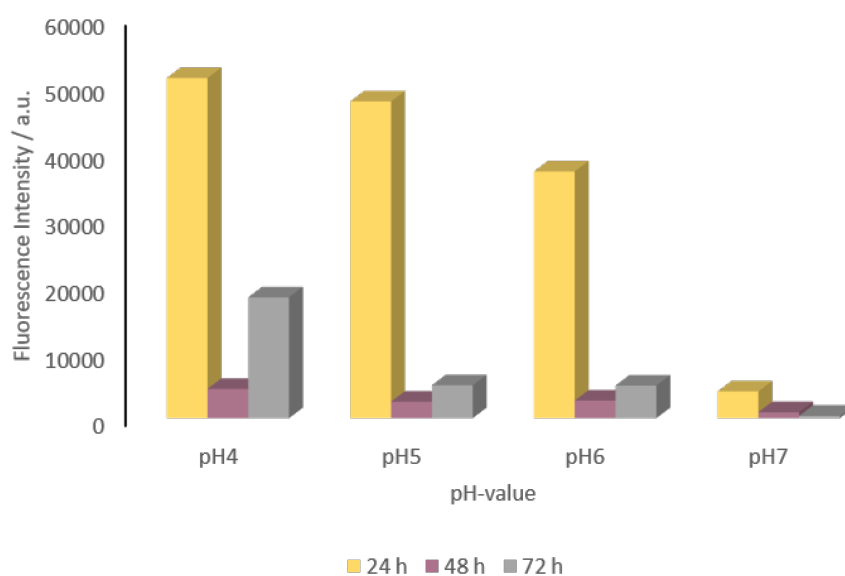
Figure 3.3: Measured fluorescence intensity after incubating CEFEFEF peptide in Milli-Q water at different pH values and for 24 h (yellow), 48 h (purple), and 72 h (grey).

As can be seen in Figure 3.3, the fluorescence intensity shows high values in three of the samples, which indicates the presence of fiber. Hereby all three samples were incubated for 24 h, whereas most other samples exhibit no fluorescence intensity.
It is also evident, that the fluorescence intensity increases with decreasing pH-value, showing the highest value at pH 4.
The decrease in fluorescence after 48 h incubation time could either point to the fact that there are no fibers within the solution or that a measuring error happened. As almost every sample shows no fluorescence intensity even after 72 h, except for pH 4, this indicates that the values after 48 h are not traceable to measuring errors. This would imply that already formed fibers either started to disintegrate after 48 h incubation time or form agglomerates..
To verify the presence of fiber, TEM measurement of the samples with the highest fluorescence intensities were conducted. Therefore the solution of pH 4 was measured after 24 h as well as after 72 h.
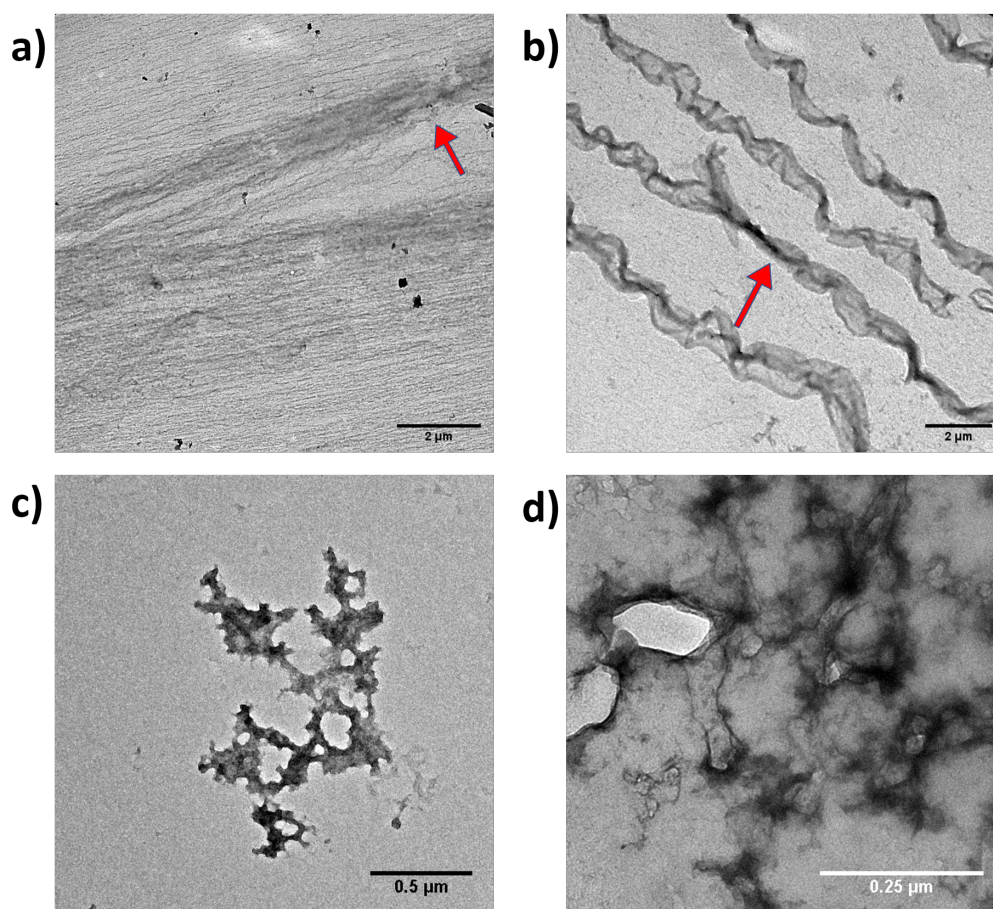
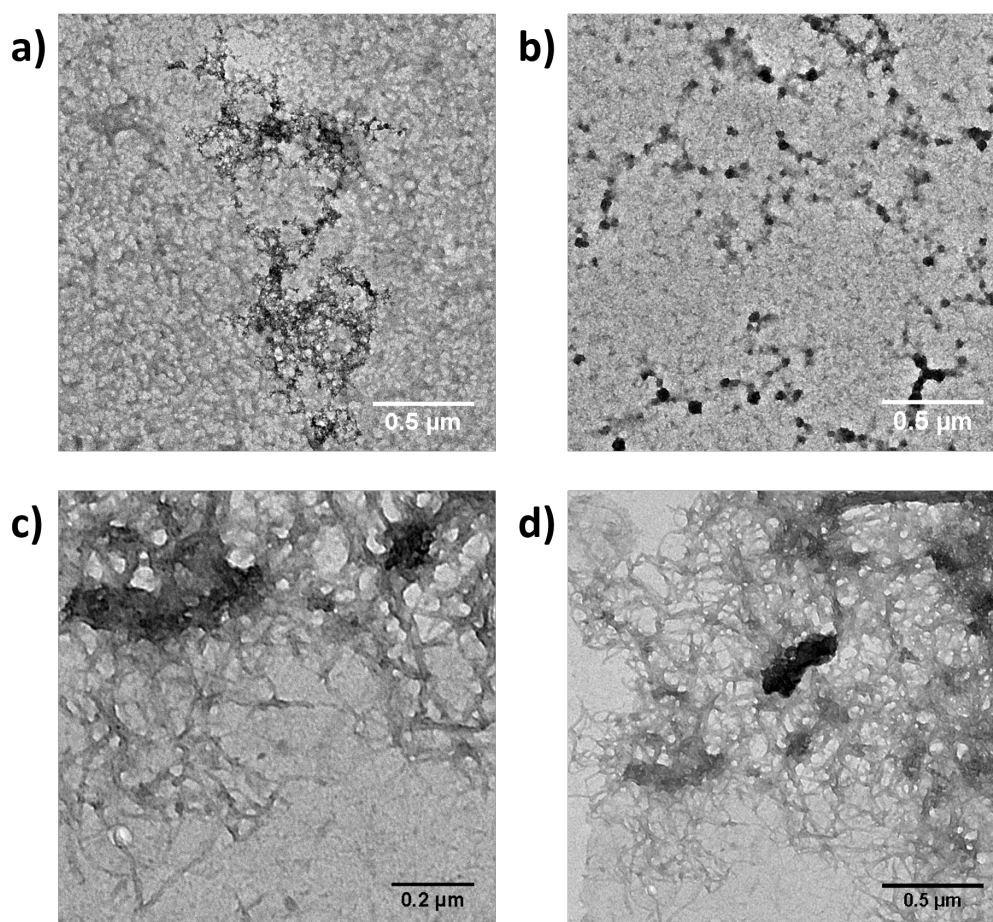Figure 3.4: TEM micrographs of CEFEFEF peptide in Milli-Q water at pH 4. **a**, **b** Show the pH 4 solution after an incubation time of 24 h. **a** The red arrow points at a fiber formation which could be the start of an assembly to a larger, fiber-like structure **b** The red arrow points at a larger fiber-like structure, which is assumed to be the result of an agglomeration of smaller fibers. **c**, **d** Show the same pH 4 solution after an incubation time of 72 h. The image shows no fibers but an agglomerate. **d** Shows a magnification of **c**.

The TEM images (Figure 3.4a and b) of the sample at pH 4 after 24 h show fibrillar, high aspect ratio structures.

Figure 3.4c and d show images of the same peptide solution, measured after 72 h. It is evident that this sample does not contain fibers but an agglomerate which seems to have an almost homogeneous structure when magnified.

Figure 3.4a and b confirm the assumptions made on the basis of the results of the fluorescence assay. It is evident that the peptide self-assembled into fibers within 24 h. Also, bigger, fiber-like structures were found on the grid (Figure 3.4b).

As Figure 3.4a seems to witness an agglomeration of the thin peptide fibers (red arrow), this suggests that the larger fibers in Figure 3.4b might showcase the end result of this process.

This finding suggests, that this peptide sequence's self-assembling behavior goes beyond forming single peptide fibers.

As Milli-Q contains no exogenous salts to shield the outer charges of the fibers, this could have caused the agglomeration to bigger fiber-like structures and after 48 h to an instability, which caused a disintegration of high aspect fibers shwon in Figure 3.4a and b. This could explain the absence of fibers in Figure 3.4c and d. Instead the images show a non-fibrillar agglomerate. This would be consistent with the results of the fluorescence assay, as the measurement at pH 4 after 72 h displayed only low intensities under the value of 40000, which was earlier defined as the threshold for 'high intensities'.

To learn more details about the larger structures in Figure 3.4b, and whether they were just drying artefacts or had already been part of the solution, dynamic light scattering as well as cryo-EM measurements could be conducted with the sample. However, these measurements could not be performed for lack of time within the framework of this thesis. Conclusively the preparation of fibers in Milli-Q water shows a time-dependeny which dramatically influences the self-assembly behavior. To learn more about this, it would be interesting to follow the self-assembly behavior of the pH 4 sample by means of TEM measurements in shorter time intervals.

3.2.2 Solvent: Sodium Chloride Solution

To screen the effect of exogenous monovalent ions on the self-assembly behavior, the following test series was conducted using sodium chloride. Therefore, six samples from the peptide in 150 M sodium chloride solution within a range of pH 2 - 7 were prepared. After an incubation time of 24 h, 48 h, and 72 h a fluorescence assay was conducted.
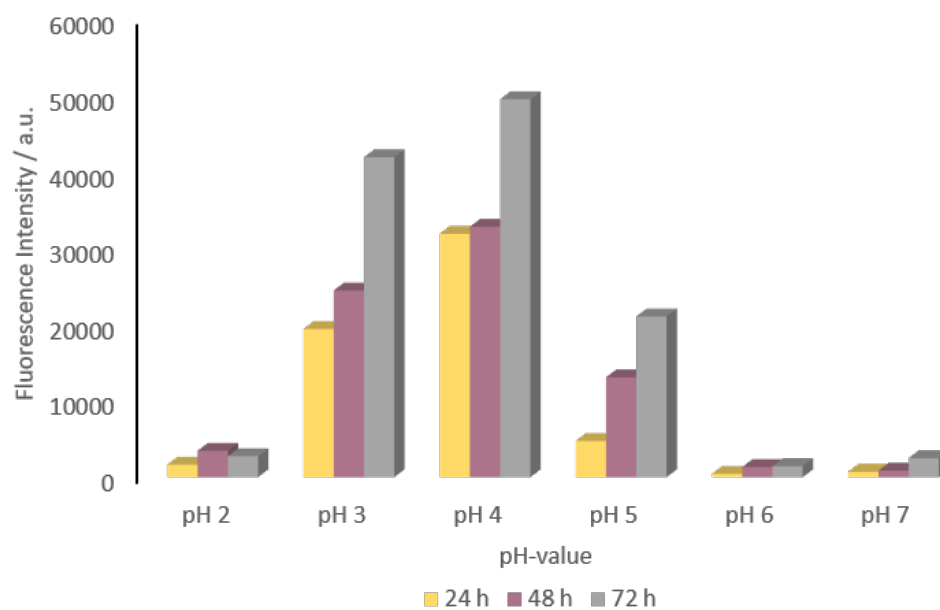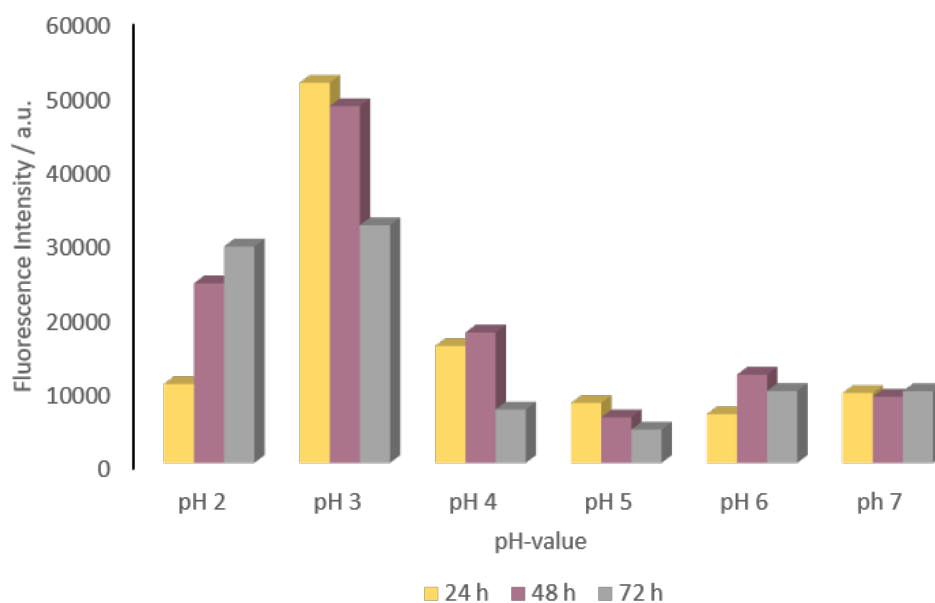

Figure 3.5: Fluorescence intensity after incubating CEFEFEF peptide in sodium chloride solution at different pH values and for 24 h (yellow), 48 h (purple), and 72 h (grey).

As can be seen in Figure 3.5, high fluorescence values are found for solutions at pH 3 and 4. Solutions at pH 3-5 show elevated levels of fluorescence intensity and therefore should contain peptide fibers, whereas pH 4 shows the highest intensity and pH 3 comparably high values. This result corresponds to the Milli-Q test series as the highest intensity was also detected at a pH of 4.

Furthermore an increase in incubation time caused an increase in fluorescence intensity, which contradicts the results from the Milli-Q testseries.

To verify the presence of fiber, TEM measurements of the samples showing the highest fluorescence intensity after 24 h and 72 h were conducted.


Figure 3.6: TEM micrographs of CEFEFEF peptide in 150 M sodium chloride solution. **a**, **b** Show the solution of pH 4 after 24 h. There are no visible fibers but agglomerates. **c**, **d** Show the solution of pH 4 after 72 h. There are visible fibers.

The TEM images shown in Figure 3.6 were taken from the sample showing the highest fluorescence intensity in Figure 3.5. Therefore, Figure 3.6a and b were taken from the sample at pH 4 after 24 h, while 3.6c and d were taken from the sample after 72 h of incubation time.

The sample after 24 h at pH 4 shows a fluorescence intesity under 40000, which indicates that the quantity of fibers is lower than in the measured sample of Milli-Q. This explains why Figure 3.6a and b show no visible fibers. Most likely the sample contains fibers but as fibers

are, compared to the size of the grid, relatively small it would take very long to locate them. Another explanation could be, that the agglomerates which can be seen in Figure 3.6a and b also cause fluorescence intensity.

In Figure 3.6c and d high aspect ratio nanofibers can be seen, which reinforces the result of the high intensity measured in the fluorescence assay: the existence of fibers is confirmed as well as the fact that an increase of incubation time led to an increase of fiber quantity.

3.2.3 Solvent: Calcium Chloride Solution

To screen the effect of exogenous divalent ions on the self-assembly behavior, the following test series was conducted using calcium chloride. Six samples from the peptide in 5 mM calcium chloride solution within a range of pH 2 - 7 were prepared. After an incubation time of 24 h, 48 h, and 72 h a fluorescence assay was conducted.

Figure 3.7: Fluorescence intensity after incubating CEFEFEF peptide in calcium chloride solution at different pH values and for 24 h (yellow), 48 h (purple), and 72 h (grey).

As can be seen in Figure 3.7, most solutions display elevated fluorescence intensities and therefore probably contain fibers.

The solutions within pH 2-4 show higher intensity levels, whereas pH 3 shows the highest values reaching levels over 40000. These results are comparable to the test series in Milli-Q water and sodium chloride solution, as they also displayed the highest intensity value at a pH of 4. Seemingly intensity values increase, the closer the pH is to 3. The same behavior was recorded for Milli-Q water and sodium chloride solution as the values increased, the closer the pH was

to 4.

Moreover, incubation time seems to not have a great impact on the self-assembling process, as the bar chart shows no specific trend within the variation of the incubation period, contrary to the results from the test series with Milli-Q and sodium chloride. For example, pH 2 shows the highest levels of fluorescence intensity after 72 h, while the sample with pH 3 shows the lowest intensity after this period. Therefore, the incubation time appears not to be decisive for the self-assembling behavior in this case.

To verify the presence of fibers, TEM measurements of the samples showing the highest fluorescence intensity after 24 h as well as after 72 h were conducted.
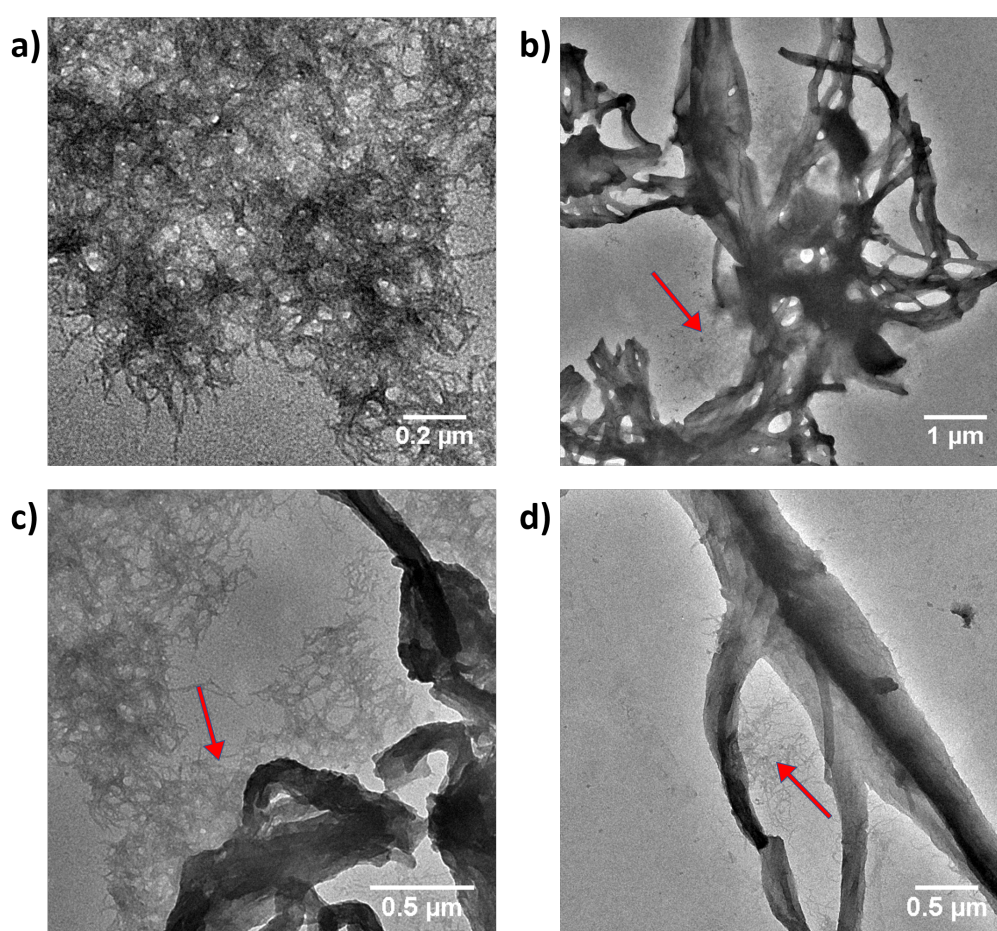

Figure 3.8: TEM micrographs of the peptide sample in calcium chloride solution at pH 3 after 24 h. **a** Shows small fibers, **b**,**c**, and **d** show bigger aggregates. Red arrows pointing at small fibers surrounding aggregates.

The TEM photographs Figure 3.8a and b show the sample at a pH of 3 after 24 h of incubation. While Figure 3.8a shows small fibers, Figure 3.8b, c, and d show bigger structures with red arrows pointing at smaller fibers surrounding the bigger structures.

Figure 3.8 confirms the assumption made on the basis of the results of the fluorescence assay. It is evident that the peptide self-assembled into fibers within 24 h. Also bigger, fiber-like

structures were found on the grid (similar to those in Figure 3.4b).

As Figure 3.8b,c, and d show a bigger structures that are surrounded by smaller fibers, this could suggest that the smaller fibers merged into bigger entities, just like the behavior of the fibers in Milli-Q Figure 3.4. This finding again suggests that, under certain conditions, higher order assemblies are formed from the peptide fibers.
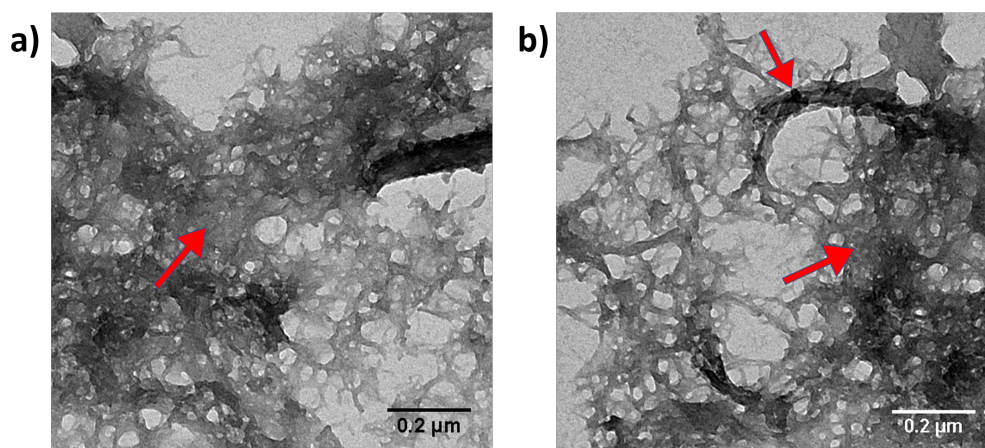
Figure 3.9: TEM micrographs of the peptide sample in calcium chloride solution at pH 3 after 72 h. **a** and **b** show small fibers as well as bigger structures. Red arrows pointing at what seems to be the merging of smaller fibers to bigger entities.

Figure 3.9 shows the same sample as Figure 3.8, but after 72 h incubation time. Here the suspected merge of small fibers is clearer. The red arrows on Figure 3.9 a and b point at what appears to be merging peptide fibers, forming structures comparable to the ones shown in Figure 3.8b. Also, there happen to be small patches of what resembles the film shown on Figure 3.3c and d which also developed after 72 h incubation time.

This behavior resemblance could again suggest, that under certain circumstances (pH value between 3-4, in Milli-Q water or calcium chloride solution) the self-assembling process exceeds the small peptide fiber stage, leading to merged fiber aggregates in the form of an even, planar film.

Dynamic light scattering as well as cryo-EM measurements should be conducted in the future with these samples, to learn more about these structures.

3.2.4 Aluminum Chloride Solution

To screen the effect of exogenous trivalent ions on the self-assembly behavior, the following test series was conducted using aluminum chloride. Six samples from the peptide in 100 mM aluminum chloride solution within a range of pH 2 - 7 were prepared. After an incubation time of 24 h, 48 h, and 72 h a fluorescence assay was conducted.
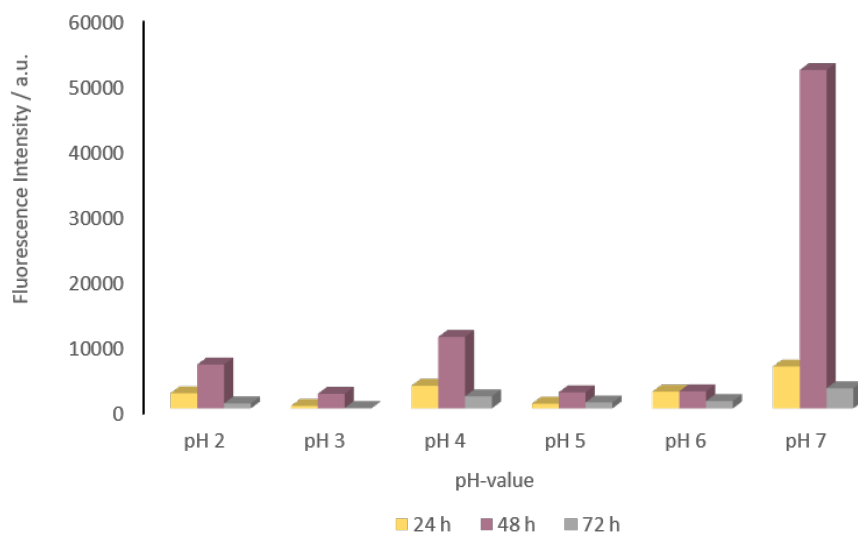
Figure 3.10: Fluorescence intensity after incubating CEFEFEF peptide in aluminum chloride
             solution at different pH values and for 24 h (yellow), 48 h (purple), and 72 h (grey).

As can be seen in Figure 3.10 the only sample that displayed high values of fluorescence in-
tensity was pH 7 after 48 h of incubation time. This is in contrast to the results from the
fluorescence assay before as they all displayed their intensity maxima around pH 3 to 4.
Furthermore, in this test series only one sample showed elevated values while the other samples
lie under or around values of 10000, which was earlier defined as 'no fluorescence'.
Thereby it is not possible to determine a certain incubation time nor pH trend within the
results.
To verify the presence of fibers, TEM measurements of the sample showing the hightest fluo-
rescence intensity after 24 h at pH 7 and 48,h also at pH 7 were conducted.
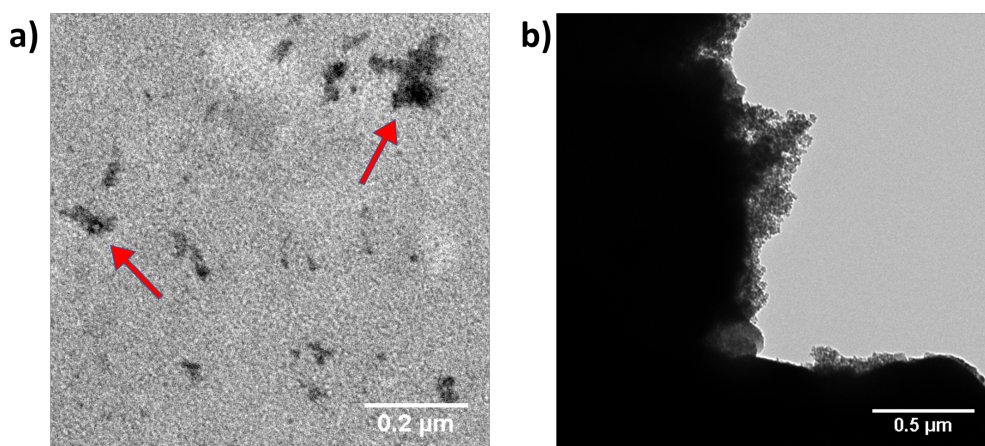
Figure 3.11: TEM micrographs of peptide in aluminum chloride solution. **a** From solution of
             pH 7 after 24 h shows no visible fiber but small agglomerates (red arrows). **b** From
             solution of pH 7 after 48 h shows a black stucture, but no visible fibers.

Figure 3.11a and b were both taken from a sample of pH 7, while Figure 3.11a was taken from the sample after 24 h and Figure 3.11b after 72 h.

Both show no visible fibers, but agglomerates.

Figure 3.11b shows a black, dense entity that covered big parts of the grid. This may be caused by a merging of the small, dense agglomerates (red arrows) from Figure 3.11a. As the fluorescence assay showed very high fluorescence intensities for the sample displayed on Figure 3.11b, there might be fibers within the dense agglomerate. Another possibility is that the agglomerates also interact with the fluorescence-causing molecule, which could explain the high levels of fluorescence measured.

3.2.5 Overview of the Test Series

The aluminum chloride solution is excluded from the following considerations, as the sample showed no fiber formation at all. This behavior could be caused by the trivalence of the added counterion. Aluminum has a strong affinity to carboxylates (Table 3.2) which is almost comparably to the affinity of protons. Furthermore, it has the ability to crosslink three fibers. The strong interaction with three peptides could cause a dense agglomeration instead of a fiber formation. This would explain why the sample (Figure 3.11b) displays a black entity covering the grid. Still it remains unclear why the test series with aluminum showed as good as no fluorescence intensity at all. As the process of self-assembly is a complex interaction of different parameters, there could be many factors that promoted this behavior.

The conducted test series unveils different coherences between the tested parameters. First of all, it is not possible to determine an ideal incubation time which applies to all solvents. There was no such trend identifiable in the bar charts.

Still it is possible to define an ideal incubation period for each of the used solvents that showed fibers. Milli-Q water showed the best results within the first 24 h and afterwards the fluorescence intensities decreased. Sodium chloride showed the best results after 72 hours, with only low fluorescence intensities in the beginning, and calcium chloride showed no preference but demonstrated good values over the entire tested incubation time.

Milli-Q water only has a minimal concentration of ions, corresponding to the least shielding of the charged groups on the surface of the fibers. This could explain the fibers tendency to disintegrate with increasing incubation time due to lack of stability.

The fact that sodium is a monovalent ion and therefore only owns the possibility to shield one of the peptide's charges at a time, but not to crosslink like the divalent calcium ion, could explain why sodium does not show the formation of neither larger fiber-like structures nor films. Calcium ions are able to crosslink formed fibers, eventually inducing the formation of a film-like structure, as shown in Figure 3.9. This assumption is further substantiated by the black entity which was obtained from the aluminum chloride solution (Figure 3.11b), as aluminum is a trivalent ion and could therefore induce the coagulation of the peptide agglomerates (Figure 3.11a) via corsslinking, potentially interfering with fiber formation.

Furthermore, the sodium chloride solution only displayed fiber formation after 72 h, while the calcium chloride solution already displayed fibers after 24 h. This could correlate with the primary stability constant of the sodium- and calcium ions as ligands for carboxylate, listed in Table 3.2, and therefore influence the kinetics of the fiber formation. Sodium shows only little affinity to carboxylate groups and therefore the charge-shielding process is probably kinetically inhibited, which would explain why the self-assembly behavior increases with increasing incubation time.

The primary stability constant of calcium is higher and additionally calcium is a divalent ion. Therefore, the interaction with the peptides carboxylates is not just kinetically, but also thermodynamically preferred, which is why the self-assembly behavior was already triggered after 24 h of incubation time and remained elevated throughout the test series.

Conclusively, it can be said, that each solvent has a characteristic way of effecting the self-assembly behavior of this peptide.

Table 3.2: Primary stability constants $(\text{Log}K_1)$ for CH_3COO^- ligands. Higher values implicate a higher affinity and stability.[44]

Ions	$\text{Log}K_1(\text{CH}_3\text{COO}^-)$
Na^+	-0,07
Ca_2^+	0,44
Al_3^+	3,13
H^+	4,76

Another finding concerns the influence of the pH value on the behavior of self-assembly. The trend of the fluorescence assay with Milli-Q water shows that the highest values of intensities were reached when the solution had a pH of 4. Sodium chloride solution displays the same behavior of the highest intensity at lower pH values, which is also reached at a pH of 4, whereas it displays no fluorescence at pH 2. Calcium chloride reached its highest intensity at a pH of 3. All solutions that contained high aspect ratio nanofibers, displayed their highest intensities at pH 3 to 4. Interestingly the theoretical isoelectric point of the peptide is exactly in that area, namely at pH 3.47.[45] Therefore, it could be possible that the quantity of self-assembly and the isoelectric point correlate. This would accord to the DLVO theory, that states that self-assembly behavior is encouraged when the system is statistically neutral,[42] even without exogenous salts. As the isoelectric point is defined as the point where the peptide is electrically neutral due to carrying no net charge, this answers the criteria for self-assembly according to the DLVO theory. As the applied pH during the test series never reached the exact value of the isoelectric point at pH 3.47, the exogenous salt helped to stabilize the peptide by shielding the few charges it had at pH 3 and 4. The test series using Milli-Q water proved that counterions are not necessary for the self-assembly process itself but for the stabilization of the formed fibers. At the isoelectric point, the peptide would probably not need any exogenous salts to stabilize the formed fibers.

The observed behavior leads to hypothesizing that the quantity of self-assembly might in general correlate with the isoelectric point of a peptide. Tho our knowledge this assumption has not been presented in literature yet.

To summarize, the initiation of self-assembly was successful. It was possible to obtain fibers with different cations and learn which conditions promote the self-assembling process.

3.3 Inducing Hydrogelation

For the establishment of aligned supramolecular coatings from the obtained high aspect ratio nanofibers, a method to preserve the achieved alignment had to be figured out first. Inspired by the works of Stupp *et al.* and Feringa *et al.* a fixation of the aligned fibers in form of a hydrogel was considered, which includes the advantage of biocompatibility.

One option to trigger hydrogelation is by adding suitable counterions to the peptide solution. The ability to form hydrogels by adding certain counterions derives from screening the inter-fibrillar repulsive forces generated by the carboxylate surface charges (double-layer potential) of the negatively charged peptide fibers.[42], [46]

Therefore a counterion had to be identified experimentally, providing the ability to form hydrogels from the peptide solution. As carboxylates have a strong affinity to some metal cations (Table 3.2), sodium-, calcium-, as well as aluminum ions were chosen to be examined as potential fixators.[46]

For this purpose an optical examination was conducted: $10\,\mu L$ samples of the peptide solution $(0,001\,M$, Milli-Q, pH 4, 24 h incubation time), which was proven to contain fibers, were mixed with $1\,\mu L$ of the solutions listed in table Table 3.3 on Parafilm.

It was examined whether the mixed solutions showed increased viscosity or turbidity.
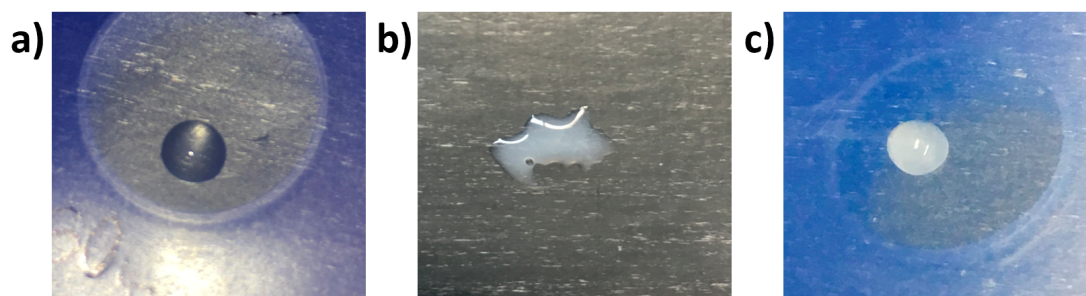
Figure 3.12: Images of the optical examination of the hydrogelation properties of of the 0.001 M CEFEFEF peptide solution with **a** 0.1 M sodium chloride solution, **b** 0.1 M calcium chloride solution and **c** 0.1 M aluminum chloride solution.

Table 3.3: Overview of the results of the optical examination shown in Figure 3.12 of the hydrogelation properties depending on the applied saline solutions.

	Solutions	Concentration	Turbidity	Viscosity	Wetting degree
a	Sodium chloride	0.1 M	X	X	X
b	Calcium chloride	0.1 M	√	√	√
c	Aluminum chloride	0.1 M	√	X	X

Figure 3.12 shows the images of the optical examination of the hydrogelation properties using different saline solution while Table 3.3 shows the results. Figure 3.12a shows the mixture of the peptide with sodium chloride solution. It is evident that neither turbidity nor a distinct wetting behavior can be determined. Figure 3.12b shows the mixture with calcium chloride solution which shows a strong turbidity and, compared to Figure 3.12a a distinct wetting behavior. Figure 3.12c shows turbidity but no observable wetting behavior.

The mixture of the peptide- and the calcium chloride solution showed the most significant changes: turbidity as well as an increase in viscosity could be observed. Furthermore a higher wetting degree of the hydrophobic Parafilm, on which the mixture was applied, was witnessed. The change in wetting degree could be explained by calcium ions successfully screening the charges on the fibers' surfaces, increasing the fibers' statistical neutrality. Therefore the lipophilicity of the mixture was elevated which led to decreased repulsion between the Parafilm and the solution. Mixtures with sodium- or aluminum chloride solution did not show the same behavior.

Also an experimental setup by Stupp *et al.* was recreated by injecting a 0.01 M peptide solution directly into a 0.1 M calcium chloride solution, with the intention to create a hydrogel-wire.[34]
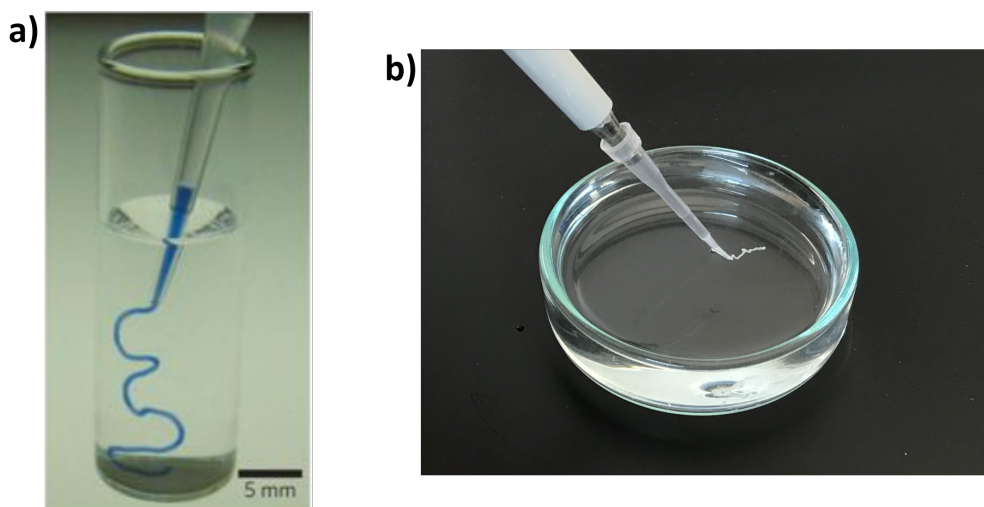
Figure 3.13: Creating hydrogel-wires. **a** Colored peptide amphiphile solution injected into phosphate-buffered saline by Stupp *et al.*[34] **b** 0.01 M Peptide solution from CE-FEFEF and Milli-Q water injected into 0.1 M calcium chloride solution.

This replicated experiment, shown in Figure 3.13, confirmed the first assumption made on the basis of the optical examination: the peptide with the sequence CEFEFEF forms a hydrogel in the presence of calcium chloride. The peptide string showed no mechanical strength, but fragmented easily which is why isolation and analysis were impossible. The lacking mechanical strength could be the result of too weak attractive interactions between the fibers, caused for example by an insufficient length of the formed fibers.

This experiment showed no success using sodium or aluminum as counterions to induce hydrogelation.

The outcome of the experiment using sodium ions, shown in Figure 3.12a and Table 3.3 as well as the unsuccessful attempt to create a hydrogel wire is not surprising, due to sodium's negative value of the primary stability constant as a ligand for carboxylate, shown in Table 3.2.[44],[46],[47] This value indicates, as explained before, that it is energetically more favourable for sodium ions to remain in solution, rather than bind to the carboxylate, as opposed to calcium- and aluminum ions. Furthermore sodium is a monovalent ion and therefore only shows low charge-screening ability, in contrast to divalent or trivalent counterions.[47]

As explained in the DLVO theory, screening the interfibrillar repulsion providing charges is necessary to enable attractive van der Waals forces to promote particle coagulation, which is concatenated to the onset of hydrogelation.[42],[47]

Furthermore, the empirical Schulze-Hardy rule states, that the threshold value for screening the double layer potential is proportional to the inverse sixth power of the counterion's valence.[46] This means that polyvalent ions should provide better charge-screening abilities and therefore enable assembly more effectively than monovalent ions, which explains why calcium forms better hydrogels than sodium.

Additionally, sodium is, due to its monovalence, not able to crosslink different fibers with each other, which would be essential for the formation of a hydrogel.

However aluminum should, for the same reason, show even better results concerning hydrogelation than calcium, as it has a higher K_1 value (Table 3.2), and it is a trivalent ion.

Contrary to the expectations based on the theories mentioned above, aluminum exhibited poor hydrogelation abilities shown in Figure 3.12c and Table 3.3, as well as an absence of fibers as can be seen in Figure 3.11.

A potential reason for the unexpected outcome of both experiments might be the tendency of aluminum to polymerize into polycations, which reduces the effective concentration that is available to bind to the carboxylates.[47] Furthermore, the process of self-assembly is a sequence of multiple complex interactions. Therefore, the outcome of an experiment can be influenced by many different, even unpredictable, parameters so that a theory is never universally valid.

For further experiments, calcium chloride was applied as the fixator agent to preserve the alignment within a hydrogel. Additionally, the Stupp group discovered that hydrogels from peptide amphiphiles using divalent cationic counterions, such as calcium ions, were non-toxic to cells, using the hydrogel as a nutrient source.[48],[49]

3.4 Methods to Induce Alignment

Inspired by the achievement of aligning peptide amphiphiles by Stupp *et al.*, this chapter deals with aligning fibers from the unmodified peptide sequence CEFEFEF and preserving the achieved alignment within a hydrogel. To verify whether the alignment of the fibers was successful, polarized optical light microscopy as well as SEM measurements were conducted. Successfully aligned peptide nanostructures as published in the literature are shown in chapter 1.6 in Figure 1.7b and Figure 1.11.

3.4.1 Alignment using Shear Forces

As the circumferential alignment of the tubes made of peptide amphiphiles by Stupp *et al.* was achieved by applying shear forces onto the peptide solution using a glass vessel with a rotatable, engine-driven rod inside Figure 1.9 the underlying concept was transferred to the simplified construction shown in Figure 3.14.
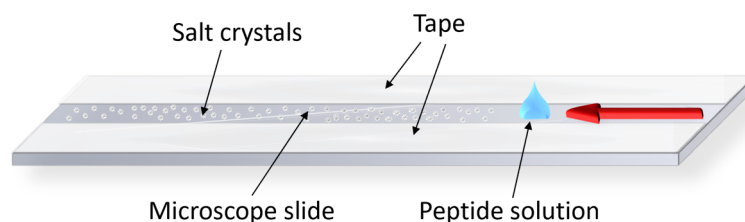
Figure 3.14: Schematic illustration of the experimental setup to create manual or automated shear forces inspired by the construction shown in Figure 1.9.

One of the setups, shown in Figure 3.14 for the experiments executed in this thesis consists of a microscope slide attached to an even surface using sticky tape. The longitudinal recess between the tapes creates a channel along the middle of the slide of approximately 0.09 mm height, as schematically represented in Figure 3.14b
Via spray coating the 0.1 M calcium chloride solution, which was identified to trigger hydrogelation, was deposited in the channel.
Shear forces were either generated manually or by means of an electric film applicator, aligning the peptide fibers within the channel. The achieved alignment was preserved by means of hydrogelation with the deposited salt crystals.

0.1 M Calcium chloride solution, which was identified to form the best hydrogels with the peptide solution, was spray coated onto the surface of the channel of the microscope slide shown in Figure 3.14, whereas a small area at the lower end of the slide was covered to prevent crystals to deposit in this region. 30 µL of 0.01 M peptide solution were deposited in this area of the cover slip. This way a hydrogelation prior to applying shear forces was prevented.

3.4.1.1 Manual Doctor Blading

For the purpose of creating coatings with highly oriented fibers, the first experiments were conducted applying manual shear forces to the 0.01 M peptide solution from CEFEFEF.

This was achieved by taking a second microscope slide and, with pressure and in a fast, uniform motion, moving it in the direction of the red arrow Figure 3.14. In doing so, the mobile microscope slide, abutted on the tape stripes, exerted shear forces on the fiber-containing liquid, along the channel in between the tape stripes.

During this process, the liquid came in contact with the calcium chloride crystals deposited in the channel, resulting in a fast hydrogelation of the applied peptide solution. One of the resulting films by means of this technique is displayed in Figure 3.15.
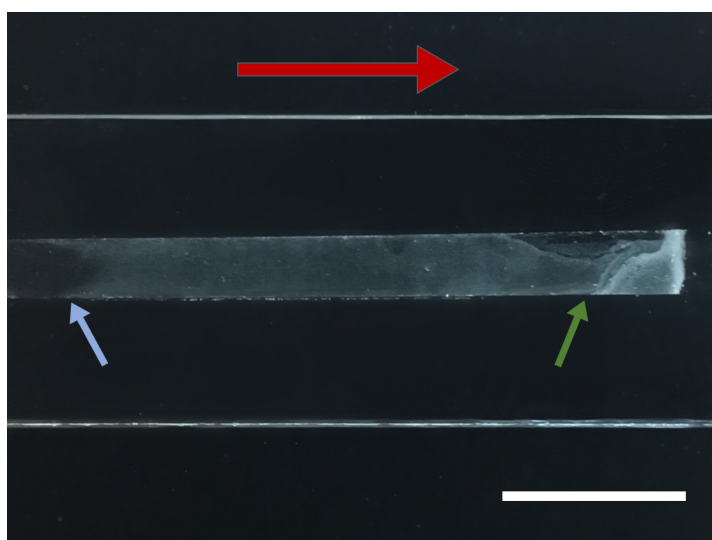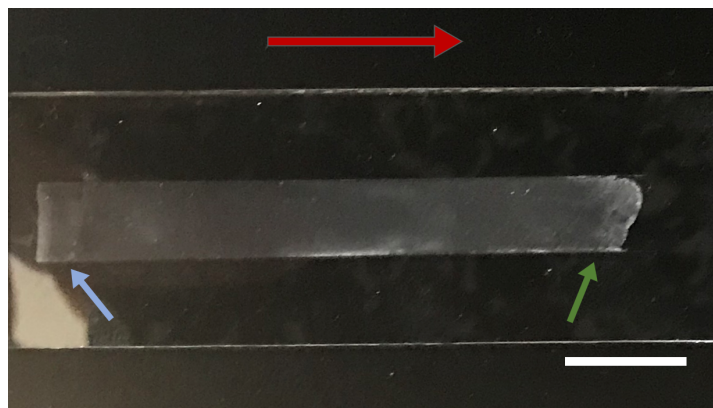

Figure 3.15: Coating generated by applying manual shear forces on the 0.01 M CEFEFEF peptide solution with 0.1 M calcium chloride solution. The red arrow points in the direction of movement, blue arrow at the initial area and green arrow at the end region. Scale bar is 1 cm.

The coating displayed in Figure 3.15 was achieved by applying manual shear forces, whereas the red arrow presents the moving direction of the exerted shear forces.

The initial area, marked by the blue arrow shows an almost fringed deposition of the hydrogel, which results from scattered salt crystals in this region. This illustrates that the hydrogelation only took place when the peptide solution came in contact with calcium ions.

The green arrow marks the end area which displays a denser material deposition, caused by excess peptide solution and salt crystals that piled up in front of the moved microscope slide. The middle segment shows an even film as the result of a homogeneous salt distribution achieved by spraycoating, as well as relatively consistent force- and speed application. Still a slight gradual increase in density can be determined, comparing the initial area and the middle segment. This is the result of the small variations in pressure and speed application, as the pressure application tended to be slightly more powerful in the beginning.

To verify whether the fibers within the film could be successfully aligned, polarized optical microscopy was performed with the sample, to identify potential anisotropic structures.
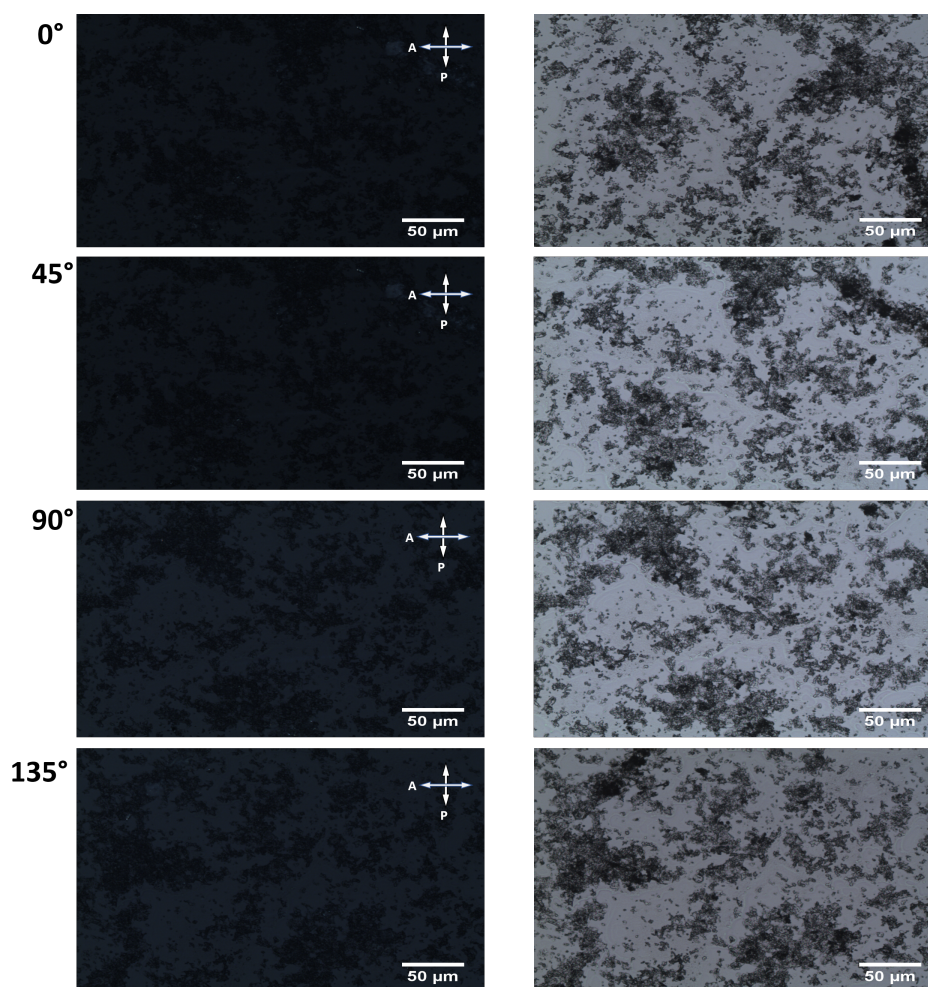
Figure 3.16: Polarized optical microscopy (l) and corresponding bright field images (r) of the manually generated coat from aqueous peptide solution and calcium chloride. Images were made under cross-polarized light and rotation of the sample by 0, 45, 90, and 135 degrees. The sample shows no birefringence at any orientation.

Since the images made under cross polarized light, shown in Figure 3.16, remained dark throughout the rotation of the sample stage, it is evident that the film shows no birefringence, as this would result in alternating birefringence colors and extinction as demonstrated in 1.11a. Moreover, the brightfield images reveal that the obtained coating is not as even as it appeared to be on the photograph from Figure 3.15, but displays a patchy distribution of the material instead. The sample did not exhibit any oriented nor anisotropic characteristics of the deposited material, indicating that the peptide fibers could not be aligned by applying manual shear forces.
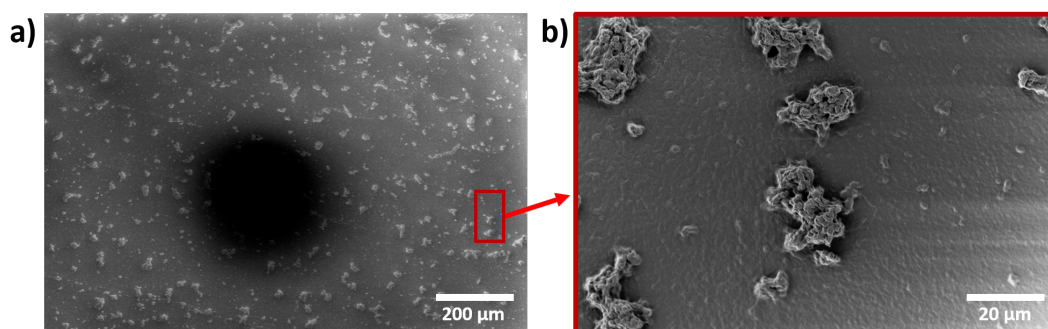
Figure 3.17: SEM micrographs of the manually generated coat from aqueous peptide solution and calcium chloride. **a** Shows the uneven distribution of the samples material while **b** shows a magnification of one of the depicted agglomerates. The sample shows no identifiable orientation.

The image Figure 3.17a shows that particles are homogeneously covering the microscope slide. When magnifying one of those particles it is evident that it does not show aligned peptide fibers but entangled agglomerates. By comparing the structure shown in Figure 3.17b with SEM micrographs from literature depicting calcium chloride crystals[50] it could be ruled out that these structures are pure artefacts from salt crsytals.

The application of manual shear forces did not bear anisotropic nor somehow oriented coatings. This could be caused by an unsteady speed and pressure during application. Furthermore, the particles seem to consist of a complex of entangled crosslinked fibers. Therefore a more complex method of aligning the fibers was tested.

3.4.1.2 Automated Doctor Blading

Another option to create coatings was by means of an automated film applicator (Figure 3.18) which applied shear forces at the same time. This method offers the advantage of a better controlability and reproducibility concerning constant speed and pressure application.

Figure 3.18: Photography of the used automated film applicator.

For the procedure the applicator with doctor blade shown in Figure 3.18 was used.

The underlying concept of shear force application remained the same as for the manual application, as well as the preparation of the microscope slide shown in Figure 3.14. Except the moving microscope slide exerting shear forces in the first setup, was exchanged for a heavy weight which would not require further manual pressure application. The weight was generated by a polished glass block of 870 g, which served not just as the pressure exerting medium but also as the doctor blader. The glas block was moved with a uniform speed of 25 mm/s, spreading the peptide solution unidirectional along the channel in between the tape stripes on the microscope slide.

Figure 3.19: Coating fabricated by applying automated shear forces on 0.01 M CEFEFEF peptide solution with 0.1 M calcium chloride solution. The red arrow points in the direction of movement, blue arrow at the initial area and green arrow at the end region. Scale bar at 1 cm.

The coating displayed in Figure 3.19 was generated by applying automated shear forces. The fabricated film is comparable to the coating obtained by means of manual doctor blading, shown in Figure 3.15, even though the coatings obtained via automated doctor blading seemed to be exhibit a slightly higher homogeneity.

Again the red arrow presents the moving direction of the exerted shear forces, while the blue arrow marks the initial area. It's evident that, in contrast to the film obtained by applying manual shear forces, the inital part shows a distinct edge. This could be caused by a more even spray coated layer of salt crystals, but also by a more uniform motion und pressure exertion.

Furthermore, there is no obvious change in the amount of deposited material along the doctor blading direction, as was previously observed in Figure 3.15.

The green arrow points at the end region. Compared to the previous coating this area is smaller and does not show as much piled up material. This is probably also caused by a more consistent, uniform motion and pressure exertion of the automated device compared to the human movement.

For verification if the fibers within the hydrogel were aligned, polarized optical microscopy was performed, to identify potential anisotropic structures.
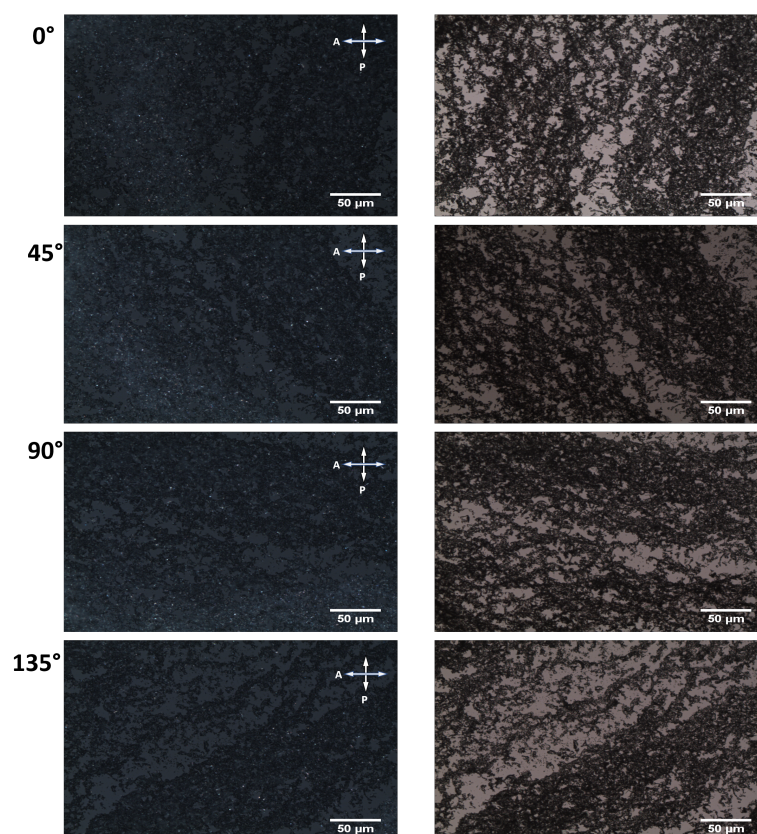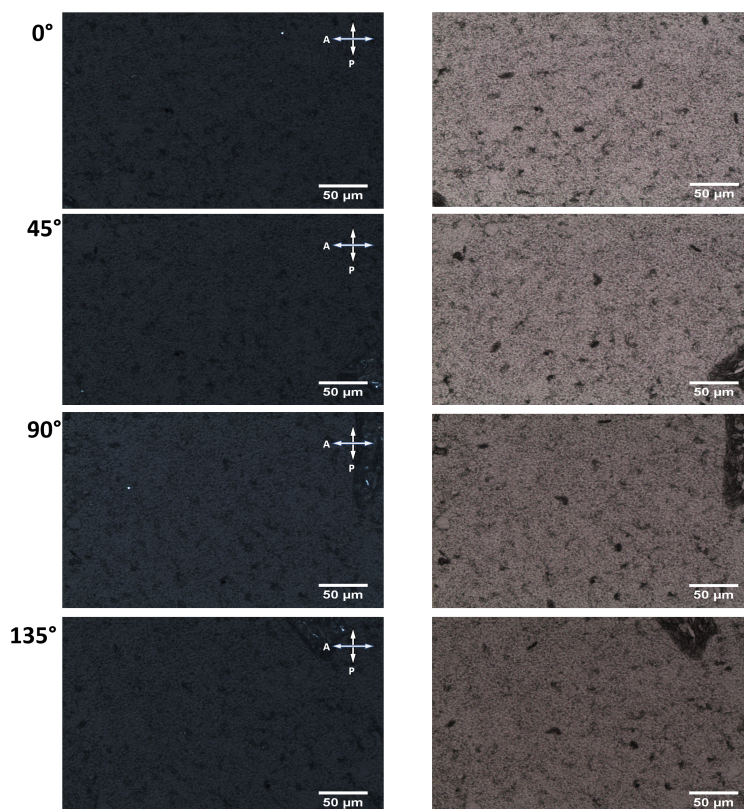
Figure 3.20: Polarized optical microscopy (l) and corresponding bright field images (r) of the coat generated by means of automated film applicator from aqueous peptide solution and calcium chloride. Images were made under cross-polarized light and rotation of the sample by 0, 45, 90, and 135 degrees. Little spots within the sample, most likely calcium chloride crystals, display birefringence, the rest of the sample does not.

Again the cross polarized images shown in 3.20 remained dark throughout the rotation of the sample stage. It is evident that the material shows no birefringence. Therefore the tested sample shows no anisotropic characteristics which proves that the peptide fibers could not be aligned into anisotropic systems by applying mechanical shear forces with the two tested methods.

Little spots within the images show birefringence, most likely originating from remaining calcium chloride crystals, which contain highly anisotropic domains as calcium chloride crystalizes in a non-cubic deformed rutile structure which therefore shows birefringence.[51] This could be explained by the fact that the calcium chloride solution was spray coated onto the microscope slide. However, it was not possible to exactly regulate the amount of solution that settled on the slide. Therefore, it is possible that a larger amount of the spray settled onto the cover slide. This would result in a higher concentration of ions, which could interact with a limited number of carboxylates. Therefore, it is possible that the excess ions, which did not interact with any carboxylates, recrystallized and appeared as the observed sources of birefringence.

Nevertheless, it is evident that the brightfield images shown in Figure 3.20 exhibit a more con-

sistent distribution of the deposited material, in an almost linear arrangement with a preferred orientation following the direction of movement, in contrast to the brightfield images as can be seen in Figure 3.16.

Furthermore, SEM measurements were conducted to take an exact look at the fibers orientation and dispersion within the film.
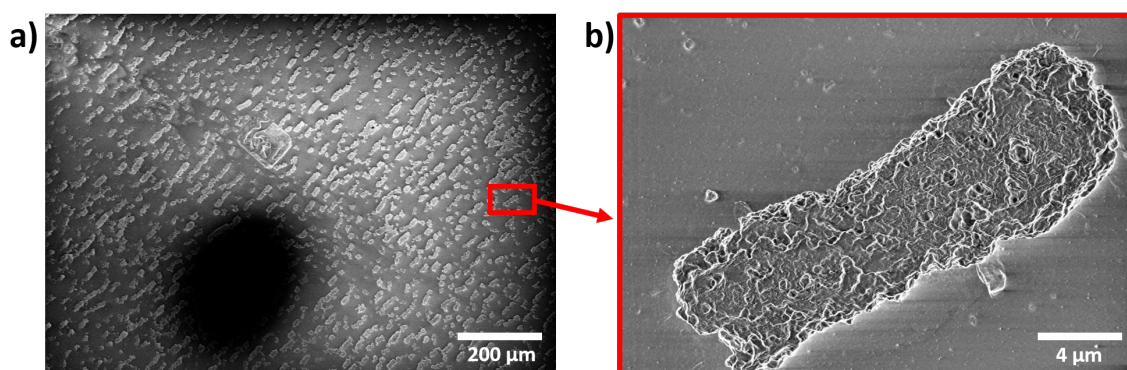
Figure 3.21: SEM micrographs of the coating generated by means of the automated film applicator from aqueous peptide solution (0.01 M) and calcium chloride solution (0.1 M). **a** Shows that the distribution of the sample is still uneven although the particles show a preferred orientation. **b** Shows a magnification of one of the depicted, cylindrical agglomerates.

Figure 3.21a shows that similar looking particles are homogeneously covering the microscope slide. When magnifying one of those particles it is evident that it does not display the structures of aligned peptide fibers but entangled, cylindrical agglomerates.

Taking the size of these structures into account they measure approx. 19 μm in length. The fibers detected in the peptide solution (MilliQ, pH 4, 24 h) also displayed longer dimensions (approx. 8 μm). Therefore, it is very likely the the entangled structures shown in Figure 3.21b were caused by an agglomeration of the fibers shown in Figure 3.4a and b.

All entangled particles in this sample display a similar morphology. Furthermore, it seems as if these cylindrical structures show a preferred orientation: all of the short sides of these particles are facing the same direction.

This almost homogeneous dispersion, as well as the orientation of the structures found on the microscope slide must be the results of a more consistent pressure as well as speed application, caused by the automated device.

Nevertheless, this method was not able to bring forth anisotropic coatings that could be verified by polarized optical microscopy.

3.4.2 Alignment using Zone Casting

Zone casting was introduced as a new method for aligning peptide fibers, as it offeres a way to create oriented, anisotropic coatings from dissolved substances.[39] The substance, in this case

the 0.01 M peptide solution, was cast onto a microscope slide which had previously been spray coated with a layer of calcium chloride.

The peptide solution was continuously supplied by a nozzle onto the moving microscope slide (Figure 1.10). Capillary forces orient the molecules provided by the meniscus during the deposition, whereas they come in contact with the previous deposited calcium chloride which leads to a hydrogelation, preserving the achieved orientation.

A test series was established with the purpose of identifying the best combination of the four variables to create coatings (Appendix, 6.0.1). Therefore, the syringe speed was varied between 15-70 µm/s, the substrate speed between 5-100 µm/s, the solution temperature between room temperature and 70 °C, and the substrate temperature between room temperature and 100 °C. First of all the parameters were varied until a certain trend or preference was identifiable. All of the obtained coatings prepared during the test series (Appendix, 6.0.1) did not show an even deposition of the material, which made it difficult to determine 'ideal' conditions. Nevertheless, it became evident, that high temperatures (over 80 °C) and high speed values (over 20 µm/s) caused an instability of the meniscus. However, low speeds (under 10 µm/s) caused the devices motor to stop. Too low temperatures (under 40 °C) led to a lack of evaporation of the solvent in the meniscus area, which caused slurring of the deposited material.

The best results were found with the parameters listed in Table 3.4, whereas further values that were found to create 'good' coatings are marked in Table 6.1, which can be found in the appendix.

Table 3.4: Parameters of the best obtained coatings during the test series.

	syringe speed	substrate speed	solution temperature	substrate temperature
Values	15 µm/s	20 µm/s	50 °C	70 °C

Coatings obtained by these parameters are discussed in the following.
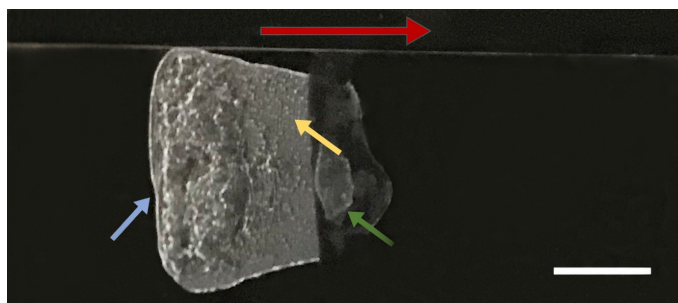
Figure 3.22: Photograph of the coating generated by means of zone casting from 0.01 M CE-FEFEF peptide- and 0.1 M calcium chloride solution by the parameters listed in Table 3.4. The red arrow points in the direction of movement, blue arrow at the initial area, green arrow at the end region, and yellow arrow points at piled-up depositions of the casted material. Scale bar is 1 cm.

The coatings obtained by means of this method (Figure 3.22) did not look as even as the coatings depicted in Figure 3.15 and Figure 3.19.

The red arrow points in the direction of movement, while the blue arrow marks the initial area. It is evident that in this area the deposited material is very patchy and uneven as this is where the liquid touched the surface and had to form a stable meniscus first. The yellow arrow points at the area where the meniscus was stable and an almost even film was established. Still the material shows piled-up formations as a result from the cogging motor. As the peptides were dissolved in Milli-Q water, the evaporation of the meniscus took too long, due to slow evaporation of water compared to highly volatile organic solvents. Therefore, the speed of the motor had to be set to such low velocity that it was not able to run smoothly anymore, which resulted in a cogging motion of the microscope slip. Hence, it was not possible to generate even coatings with the current setup. The green arrow marks the end zone of the process.

Figure 3.23: Polarized optical microscopy (l) and corresponding bright field images (r) of the coat generated by means of zone casting from aqueous peptide solution and calcium chloride. Images were made under cross-polarized light and rotation of the sample by 0, 45, 90, and 135 degrees. The sample shows small spots of birefingence, most likely caused by calcium chloride crystals. The rest of the sample does not show any birefringence.

The samples obtained from zone casting did not show birefringent characteristics as evident from Figure 3.23 indicating the absence of anisotropic coatings from zone casting.

Compared to the structures that could be seen in the brightfield images of Figure 3.16 and Figure 3.20 the brightfield images do not display any definable structures. Therefore, it is not possible to identify any kind of orientation.

To verify whether the fibers within the piled-up material deposition could be successfully aligned, polarized optical microscopy was performed with the sample, to identify potential oriented structures.
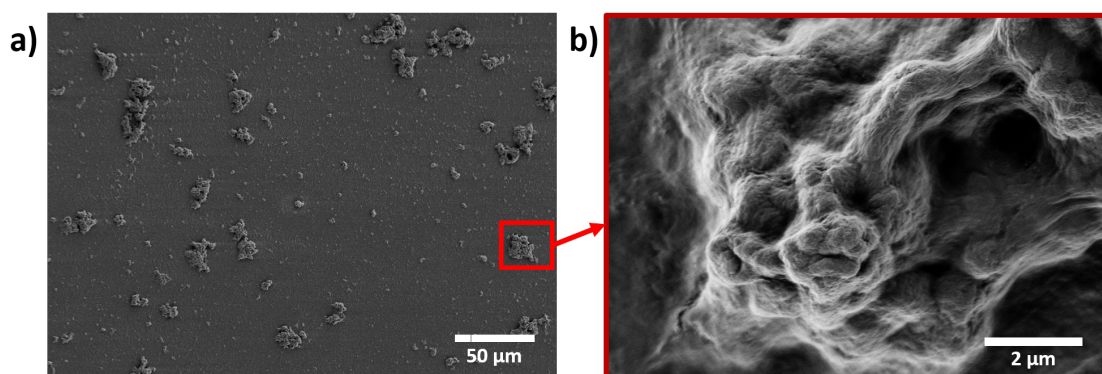
Figure 3.24: SEM micrographs of the coat generated by means of zone casting from aqueous peptide solution and calcium chloride. **a** Shows a random distribution of the material on the microscope slide. **b** Shows a magnification of one of the agglomerates.

The conducted SEM measurements proved that there was inhomogeneous deposition of the material occuring on the microscope slide during zone casting , as shown in Figure 3.24a. The magnification (Figure 3.24b) of one of the particles displayed in Figure 3.24a showed that the fibers within the solution did not form agglomerates of a certain, recurring shape, as the cylindrical particles in Figure 3.21 or the SEM micrograph showcasing the pursued structure shown in Figure 1.11 did.

Under the given conditions, the technique of zone casting could not deliver the intended results of homogeneous coatings nor an alignment of the components. A reason for the outcome could be that water, with its relatively low vapor pressure, was used as a solvent for the peptides. Further experiments could be conducted using a solvent with a lower boiling point if it is possible to identify an organic solvent that allows the formation of fibers and the subsequent hydrogelation with counterions. Another possibility would be to modify the zone casting device to overcome the stop-go motion. Herefore the device would have to be equipped with a better drive.

3.4.2.1 Overview of the Alignment Results

The methods applied in this thesis to achieve an alignment of the peptide fibers did not display the desired results as depicted in Figure 1.11 yet. However, the most promising method seems to be the automated application of shear forces since the material exhibited a recurring, almost uniform length-width-ratio of the deposited material, even though this ratio was still not as

distinct as it was in the results shown in Figure 1.11. Since it was not possible to achieve
an orientation on the microscale, the results from polarized optical microscopy confirmed the
absence of anisotropy on the macroscale, while a certain orientation was identifiable in the
brightfield images Figure 3.20. Further alignment experiments could be conducted trying the
other parameters that were identified to promote self-assembly of this sequence, such as the
peptide in calcium chloride solution at pH 3 after 24 h incubation time.

Another consideration would be to try more invasive methods for aligning the fibers as they
otherwise appear to be entangled in solution, due to potential cross linkage between the fibers.
Therfore, an alignment using stronger shear forces, for example by using the construction of
Stupp *et al.* shown in Figure 1.9 should be considered. Another idea would be the alignment
within a magnetic field following the idea of De Laporte *et al.*.[32]

4 Conclusion and Outlook

Recapitulating the present thesis, it can be stated that the synthesis and purification of the peptide with the sequence CEFEFEF, as well as its characterization were successful.

Furthermore, various conditions influencing the peptide's self-assembly behavior were screened by means of establishing a test series. Different parameters were identified, that were either inhibiting or promoting the inherent predisposition of this sequence to self-assemble. Thereby the tendency of the peptide to display the highest self-assembling behavior at its isoelectric point could be observed. This leads to the hypothesis that this finding might be transferable to SAPs in general.

Additionally, it was possible to induce a hydrogelation of the self-assembled peptides, which was achieved by screening the peptide's charges with a suitable counterion.

Also, the fabrication of homogeneous coatings was achieved, even though these coatings did not exhibit the desired macroscopic alignment.

Due to the potential bioactive qualities of the synthesized peptide and its ability to form hydrogels, the sequence shows great potential for future biomedical applications, such as 3D cell cultures. An alignment of the fibers within this hydrogel could for example be of great use in the field of neuroscience and tissue regeneration.

The alignment of this peptide, and SAPs in general, should therefore be further investigated by means of other methods, as the methods applied in this thesis were possibly not suited to achieve the desired alignment.

Therefore, a modification of the peptide sequence should be taken into consideration, by implementing a lipophilic amino acid side chain into the peptide. This idea is inspired by the general structure of peptide amphiphiles but, as to having only amino acids within the 'chain', the inherent biological origin would be maintained. Amino acids like isoleucine and valine would be, due to their high hydrophobicity compared to the other amino acids, preferred candidates for this approach. This could be a potential pathway to create longer high aspect ratio nanofibers. Moreover, the fixation of potential alignment could be optimized by implementing components that can covalently crosslink fibers. To maintain the inherent biological origin of the sequence, this might be achieved by integrating more cysteines into the peptide, as these have the ability of forming cystines, covalently linking peptides to one another.

Furthermore, a continuative idea for obtaining anisotropic coatings from peptide sequences could for example be the adaption of the idea of a circumferentially turning rod, exhibiting significant shear forces and thereby facilitating the anisotropic arrangement of the peptide

fibers. The following schematic construction could be applied for further experiments.
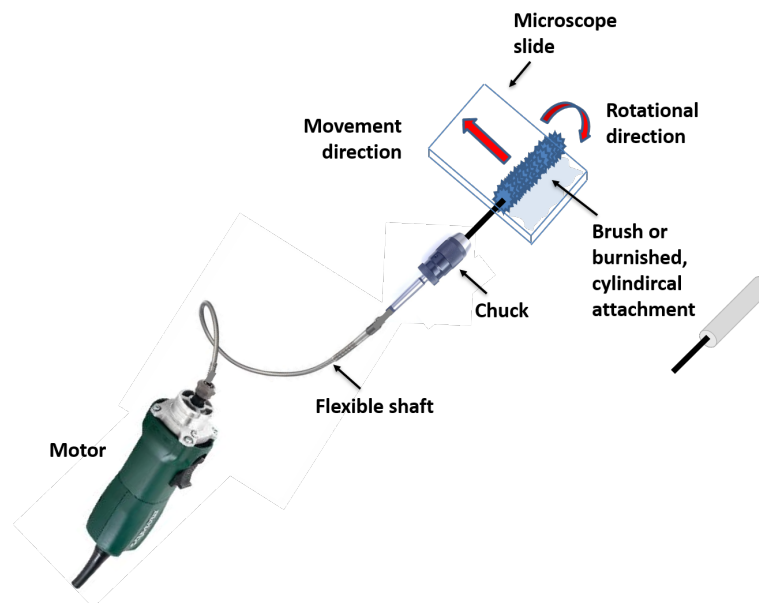
Figure 4.1: Schematic illustration of the conceived construction for further alignment exper-
iments. The construction consists of a motor, for example from an electric drill
with an attached flexible shaft.[54]–[56] At the end either a brush or a burnished,
cylindrical top unit is installed, carrying out the rotary motion of the motor?

However, a fundamental change of the aligning method should also be taken into consideration,
since other methods presented in literature displayed success in orienting fibers, such as by
means of a magnetic or electric fields.

Furthermore, the effect of the isoelectric point on the self-assembling behavior should be exam-
ined more thoroughly, also concerning its impact on the length of resulting fibers, as it offers a
way to predict the properties of the peptide by way of calculation. This could be approached
by establishing a test series with a variety of SAPs, monitoring their self-assembling behavior
around the pH value of their isoelectric point.
Further findings in this area would be very interesting for drug delivery systems, as it would
allow a more targeted design of SAP hydrogels for medical applications. The self-assembling
behavior could be "adjustable" by adding amino acids lowering or elevating the value of the
isoelectric point. This way the field of pH-sensitive SAPs with isoelectric points at physiologi-
cal pH value would be better controllable, improving pH-sensitive hydrogels for drug delivery
systems.

5 Experimental

5.1 Chemicals

Unless stated otherwise, all reagents and chemicals were obtained from commercial suppliers.
In case further purification was required it is specified accordingly.

The water used was demineralized beforehand.

Only solvents with the declaration 'for peptide synthesis' were applied during the peptide synthesis .

5.2 Solid-phase peptide synthesis (SPPS)
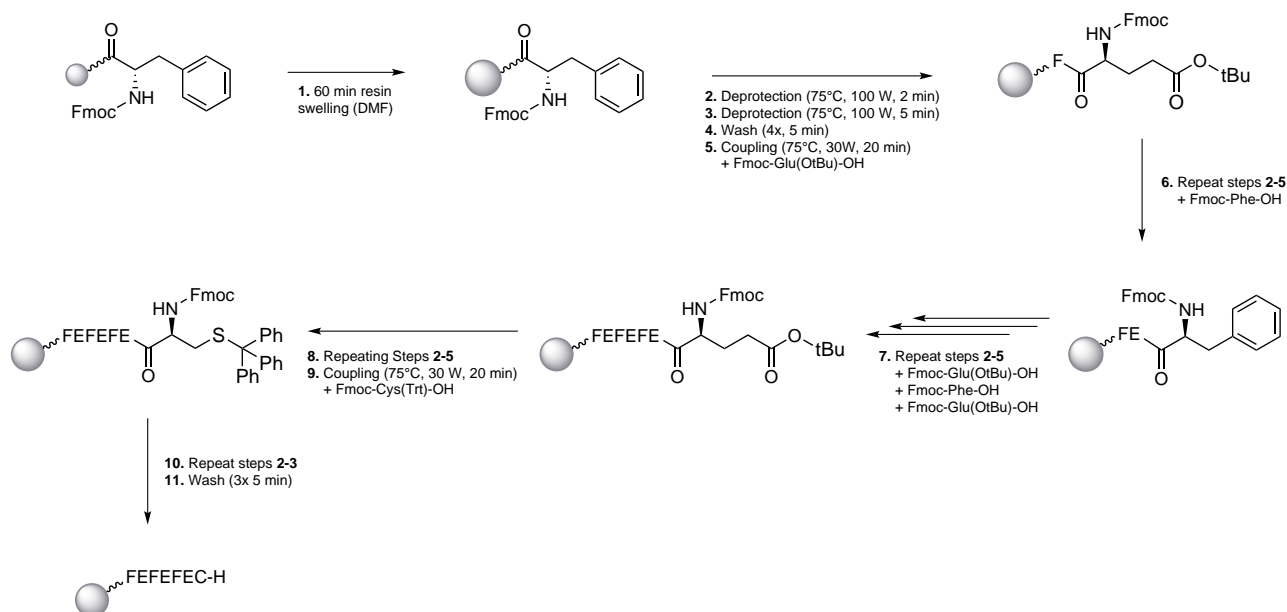
Figure 5.1: Schematic illustration of the performed solid-phase peptide synthesis.

The first step of the SPPS required the resin (0.065 mmol/g, 0.5 mmol, 0,769 g, 1 eq.) to swell in DMF (12 mL) for an hour. The consecutive synthesis was carried out using a Liberty Blue peptide synthesizer by CEM, which is an automated microwave powered model.

The respective vessels of the device above were filled with Cysteine (Fmoc-Cys(Trt)-OH,

4 mmol, 2.82 g, 2x 4 eq.), Glutamate (Fmoc-Glu(OtBu)-OH, 2 mmol, 3.07 g, 4 eq.), Phenylala-
nine (Fmoc-Phe-OH, 2 mmol, 1.86 g, 4 eq.), DMF (Solvent, 400 mL), piperidine (Deprotection,
40 mL mixed with 160 mL DMF), PyBOP (Activator, 9.4 g in 36 mL DMF), and DIPEA (Ac-
tivator base, 6.6 mL in 19 mL DMF).

After placing the soaked resin material in the designated reaction vessel of the peptide syn-
thesizer, the program was started and followed the eleven steps shown in the reaction scheme
Figure 5.1.

After completion of the program the peptide which was still linked to the resin material was
quantitavely washed out of the reaction vessel into a glass vial by adding some extra DMF.

5.3 Standard Cleavage Procedure

After the resin material had settled at the bottom of the vessel the supernatant DMF was
removed using a syringe and the remaining solvent was evaporated by carefully exposing the
material to pressurized air.

In a second vial, a mixture of TFA (1.9 mL), TIPS (0.05 mL), and Milli-Q water (0.05 mL) was
prepared and added to the resin material, resulting in severe smoke development caused by
DMF residues. The suspension was agitated for 2 hours using a magnetic stirrer.

The liquid phase containing the peptide was isolated using a pasteur pipette and the remaining
resin material washed once by adding pure TFA (3-4 drops).

The peptide solution was added to chilled diethylether (20 mL) to initiate precipitation of the
peptide which was completed after 20 minutes in a freezer. The suspension was placed into
a centrifuge for 12 minutes (3800 rpm, 4 ℃). Afterwards, the falcon tube was covered with a
lintfree paper cloth and placed in a desiccator until the ether was completely removed.

5.4 Peptide Purification

After cleavage and precipitation, the peptide was purified by means of reversed-phase HPLC
(device: Shimadzu Analytical HPLC system, column: Gemini 5 um C18 110 LC Column
150 x 4.6 mm) using acetonitrile/water (0.1% ammonium hydroxide) as a mobile phase (speed:
25 mL/min).

For this purpose the peptide was dissolved in Milli-Q water (5 mg/mL). The mixture was
vortexed and placed into an ultrasonic bath (Branson Digital Sonifier®, 250-D).

Due to poor solubility of the peptide a few drops of pure ammonium hydroxide needed to be
added until a clear solution was obtained.

Before injecting the peptide solution into the HPLC, the solution was filtered using a syringe
filter (Fischerband, PTFE 0.2 µm). The filtered peptide solution was then injected through a
manual injector into the mobile phase within the first 7 min of the program.
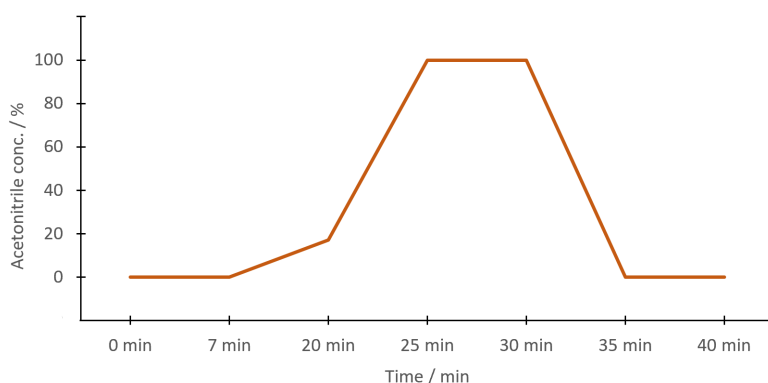
Figure 5.2: Solvent composition used for the purification of CEFEFEF peptide.

The program started with running only water as solvent for 7 min, followed by ramping up to 17% acetonitrile in 13 min and then again ramping up to 100% acetonitrile in 5 minutes. The solvent flow remained 5 min on 100% acetonitrile and subsequently ramping down to 0% acetonitrile within 5 min, remaining on 100% water until the program has finished.
The collected fractions were analysed by means of ESI-MS.

5.5 ESI-MS

In order to identify the fractions which contained the desired product, ESI-MS measurements were performed using an Advion express CMS instrument at an injection speed of $10 \, \mu L/min$. For this purpose a sample of each of the collected fractions from HPLC potentially containing the peptide, still dissolved in the mobile phase, were injected via syringe driver.

5.6 LC-MS

To verify if the purification via HPLC was successful a LC-MS measurement was performed. The freeze dried peptide was dissolved in methanol (1 mg/mL) measured with a Shimadzu LC MS 2020 equipped with an ESI source, a Kintex EVO C18 column (2.1x 50 mm, 2.6 μmeter), and a SPD-20A UV-Vis detector.

5.7 Preparation of Peptide Solutions

To induce the self-assembly of the purified peptide, a test series under variation of certain parameters was carried out. The tested parameters were: type of added counterion, pH-value, as well as incubation time.
Other than that, the sample preparation remained unchanged, enabling a direct comparison among one another. The applied technique proved to be advantageous for the subsequent TEM

measurements.

A peptide solution (0.01 M) was prepared using Milli-Q water, aluminum chloride solution (100 mM), calcium chloride solution (5 mM), or sodium chloride solution (150 mM).

By adding 0.1 M sodium hydroxide solution or 0.1 M hydrochlorid acid the pH value was adjusted, using a pH meter (Mettler Toledo MP 220 + Mettler Toledo InLab Semi-Micro pH electrode). The test series was performed trying different pH values in a range of 2-7.

After incubating the prepared solutions for 24 hours at room temperature in an Eppendorf-tube they were diluted by a factor of 10 by adding either more Milli-Q water, aluminum chloride-, calcium chloride-, or sodium chloride solution .

5.8 Fluorescence Assay

Fluorescence Assays were conducted using a Tecan Spark 20M Multimode Microplate Reader and the PROTEOSTAT® Protein aggregation assay by Enzo Life Sciences, Inc..

A solution of 10X PROTEOSTAT® assay buffer (0.35 µL), PROTEOSTAT® detection reagent (0.175 µl), and Milli-Q water (34.475 µL) was prepared.

9 µL of each peptide solution to be tested were placed on a well plate (384 Well Small Volume ᵀᴹ LoBase Polystyrol Microplate µClear®) and 1 µL of the prepared proteostat solution was added, right before the measurement.

The well plate was inserted into the microplate reader and the program was started.

After 15 minutes of incubation time in the dark while shaking at 510 rpm, the fluorescence intensity was measured with an excitation and emission bandwith of 20 nm. The excitation wavelength was set to 550 nm, followed by an emission wavelength of 600 nm.

Control measurements were conducted for each run, by measuring only the solvent medium without any added peptides.

5.9 Transmission Electron Microscopy (TEM)

TEM measurements were conducted using a JEOL JEM-1400 series transmission electron microscope operating at 120 kV accelerating voltage. 5 µL of the peptide solution (1 mM) were deposited onto a 300 mesh copper grid covered with a thin electron-transparent support film made of Formvar (R), freshly cleaned with an oxygen plasma treatment (Diener electronic Femto low-pressure plasma system), rendering the grid more hydrophilic and therefore promoting better surface wettability.

After a 4 minute incubation time at room temperature the excess solution was removed by pressing a filterpaper onto the back surface of the grid. After allowing the grid to air-dry for 10 minutes, it was further incubated for 2 minutes exposing it to 10 µL of a 4% aqueous uranyl acetate solution to achieve a positive staining. Afterwards the grid was washed three times

using Milli-Q water.[52],[53]

Images were acquired using an on axis Gatan US1000 2k CCD camera.

5.10 Alignment Experiments

Prior to use, microscopy slides were thoroughly cleaned using Milli-Q water followed by ethanol and acetone, and afterwards stored in ethanol.

For the alignment experiments an aqueous solution of CEFEFEF $(0.01\,M)$ at pH 4 was prepared and incubated for 24 h at room temperature. Just before applying the coatings, a layer of spraycoated calcium chloride solution $(0.1\,M)$ was deposited on the cover slip. In doing so, a small area at the lower end of the slide was concealed to prevent salt crystals to deposit there. In this area a drop of $30\,\mu L$ of the peptide solution was applied.

The manual shear force application was conducted using a second microscope slide as doctor blader, while the automated version used a 870 g polished glass block. For the automated alignment the film applicator Coatmaster 509 MC by Erichsen was used (Figure 3.18). For more details concerning the application itself see chapters 3.4.1.1 and 3.4.1.2. Zone Casting was conducted using the device created by Tracz *et al.*[39] and provided by the group of P. Blom at the MPIP. The device has four adjustable parameters: temperature of the solution within the syringe, temperature and speed of the substrate, and speed of the plunger of the syringe to control the speed of the liquid.

5.11 Polarized Optical Microscopy

For polarized optical microscopy imaging the samples were prepared on microscope slides by means of manual- or automated shear force application or zone casting. The microscope slide with the respective sample were imaged between two perpendicular light polarizers using a Zeiss Axiophot in reflection mode with a x10 magnification lens (Epiplan-NEOFLUAR 10x/0.30 Pol Objective) and a Leica color CCD camera. By means of a sample stage the sample could be rotated. For bright-field images the device was used without the polarizers.

5.12 Scanning Electron Microscopy (SEM)

For SEM imaging the samples were aligned as described in the chapter 7.4. The SEM images were taken using a Hitachi SU8000 equipped with an energy dispersive x-ray detector operating at an accelerating voltage of 0.1 0,7 kV.

List of Figures

List of Tables

Bibliography

[1] Grechka, V. I. Applications of seismic anisotropy in the oil and gas industry. *EAGE Publications* (2009).

[2] Schmidt, M., "Chemie verstehen: Der feste Zustand". Retrieved from $https : //www.cumschmidt.de/s_{a}ggr_{f}est.htm$

[3] Shaykhutdinov, T., *et al.* Supramolecular orientation in anisotropic assemblies by infrared nanopolarimetry. *ACS Macro Letters* **6(6)**, 598-602 (2017).

[4] Kong, W., *et al.* Muscle-Inspired Highly Anisotropic, Strong, Ion-Conductive Hydrogels. *Advanced Materials*, **30(39)**, 1801934 (2018).

[5] Kim, H. N., *et al.* Nanotopography-guided tissue engineering and regenerative medicine. *Advanced Drug Delivery Reviews* **65(4)**, 536-558 (2013).

[6] Berg, J. M., Tymoczko, J. L., Gatto Jr, G. J. Stryer: Biochemistry. *WH Freeman and Company* **7**, 306-307 (2002).

[7] Whitesides, G. M., Grzybowski, B. Self-assembly at all scales. *Science* **295(5564)**, 2418-2421 (2002).

[8] Halley, J. D., *et al.* Consistent concepts of self-organization and self-assembly. *Complexity* **14.2**, 10-17 (2008).

[9] Koutsopoulos, S. Self-assembling peptides in biomedicine and bioengineering: Tissue engineering, regenerative medicine, drug delivery, and biotechnology. *Peptide Applications in Biomedicine, Biotechnology and Bioengineering*, 387-408 (2018).

[10] Lehn, J. M. Supramolecular chemistry, *Germany: Vch, Weinheim* **Vol. 1, No. 995**, 6-7 (1995).

[11] Hartgerink, J. D., Beniash, E., Stupp, S. I. Self-assembly and mineralization of peptide-amphiphile nanofibers. *Science*, **294(5547)**, 1684-1688 (2001).

[12] Amalgam Modelmaking Ltd., Amalgam-Micelle-III for the Science and Technology Facilities Council. Retrieved from $https : //www.amalgam-models.co.uk/amalgam-micelle-iii/$.

[13] Hoffman, A. S. Hydrogels for biomedical applications. *Advanced Drug Delivery Reviews* **64**, 18-23 (2012).

[14] Caló, E., Khutoryanskiy, V. V. Biomedical applications of hydrogels: A review of patents and commercial products. *European Polymer Journal*, **65**, 252-267 (2015).

[15] Zhang S. Discovery and design of self-assembling peptides. *Interface Focus* **7**, 20170028 (2017).

[16] Merrifield, R. B. Solid phase peptide synthesis. I. The synthesis of a tetrapeptide. *Journal of the American Chemical Society* **85(14)**, 2149-2154 (1963).

[17] Bruice, P. Y. Organic chemistry. Upper Saddle River, *NJ: Pearson/Prentice Hall*, **5** (2004)

[18] Prince, E., Kumacheva, E. Design and applications of man-made biomimetic fibrillar hydrogels. *Nature Reviews Materials* **1**, (2019).

[19] Schneider, A., Garlick, J. A., Egles, C. Self-assembling peptide nanofiber scaffolds accelerate wound healing. *PloS one*, **3(1)**, e1410 (2008).

[20] Tysseling-Mattiace, V. M., *et al.* Self-assembling nanofibers inhibit glial scar formation and promote axon elongation after spinal cord injury. *Journal of Neuroscience* **28(14)**, 3814-3823 (2008).

[21] Galler, K. M., Aulisa, Hartgerink, J. D. Self-assembling multidomain peptide hydrogels: designed susceptibility to enzymatic cleavage allows enhanced cell migration and spreading. *Journal of the American Chemical Society* **132(9)**, 3217-3223 (2010).

[22] Purves, D., Augustine G.J., *et al.* Neuroscience. *De Boeck, Sinauer, Sunderland, Mass*, (2014).

[23] Ceyhun, O. Peptide-polymer-hybrid materials for advanced retroviral gene transfer agents *(Diploma Thesis, Johannes Gutenberg-Universität Mainz)*, (2018).

[24] Schilling C. *et al.* Sequence-Optimized Peptide Nanofibers as Growth Stimulators for Regeneration of Peripheral Neurons. (2019 submitted).

[25] Zhang, S., Holmes, T., *et al.* Spontaneous assembly of a self-complementary oligopeptide to form a stable macroscopic membrane. *Proceedings of the National Academy of Sciences* **90(8)**, 3334-3338 (1993).

[26] Zhang, S. Fabrication of novel biomaterials through molecular self-assembly. *Nature Biotechnology*, **21(10)**, 1171 (2003).

[27] Harris I. R., Harmon A. M., Brown L. J., Gosiewska A., *US Patent 8,039,258 B2*, (2011).

[28] Zhou, J., Xu, B. Aromatic–aromatic interactions enhance interfiber contacts for enzymatic formation of a spontaneously aligned supramolecular hydrogel. *Journal of the American Chemical Society* **136(8)**, 2970-2973 (2014).

[29] Birk, D. E., Fitch, J. M., Babiarz, J. P., Linsenmayer, T. F. Collagen type I and type V are present in the same fibril in the avian corneal stroma. *The Journal of Cell Biology* **106(3)**, 999-1008 (1988).

[30] Park, S. J., Seo, M. K. Interface science and composites (Vol. 18). *Academic Press*, 457 (2011).

[31] Sun, Z., Aida, T., *et al.* An Anisotropic Hydrogel Actuator Enabling Earthworm-Like Directed Peristaltic Crawling. *Angewandte Chemie*, **130(48)**, 15998-16002 (2018).

[32] Omidinia-Anarkoli, A., De Laporte, L., *et al.* An injectable hybrid hydrogel with oriented short fibers induces unidirectional growth of functional nerve cells. *Small* **13(36)**, 1702207 (2017).

[33] Emtiazi, G., Zohrabi, T., *et al.* Vertical Alignment of Size-Controlled Self-Assembled Diphenylalanine Peptide Nanotubes Using Polyethersulfone Hollow Fiber Membranes On Silicon. *International Journal of Peptide Research and Therapeutics*, **1-7**, (2018)

[34] Zhang, S., Stupp, S. I. A self-assembly pathway to aligned monodomain gels. *Nature Materials*, **9(7)**, 594 (2010).

[35] Li, I. C., Hartgerink, J. D. Covalent Capture of Aligned Self-Assembling Nanofibers. *Journal of the American Chemical Society*, **139(23)**, 8044-8050 (2017).

[36] Chen, J., Feringa, B. L., *et al.* Artificial muscle-like function from hierarchical supramolecular assembly of photoresponsive molecular motors. *Nature Chemistry* **10(2)**, 132 (2018).

[37] McClendon, M. T., Stupp, S. I. Tubular hydrogels of circumferentially aligned nanofibers to encapsulate and orient vascular cells. *Biomaterials*, **33(23)**, 5713-5722 (2012).

[38] Chin, S. M., Synatschke, C. V., *et al.* Covalent-supramolecular hybrid polymers as muscle-inspired anisotropic actuators. *Nature Communications*, **9(1)**, 2395 (2018).

[39] Tracz, A., *et al.* Zone casting – a universal method of preparing oriented anisotropic layers of organic materials. *Materials Science-Poland* **22.4**, 415-421 (2004).

[40] Pisula, W., Müllen, K., *et al.* A zone-casting technique for device fabrication of field-effect transistors based on discotic hexa-peri-hexabenzocoronene. *Advanced Materials* **17(6)**, 684-689 (2005).

[41] Ralhan, K., KrishnaKumar, V. G., Gupta, S. . Piperazine and DBU: a safer alternative for rapid and efficient Fmoc deprotection in solid phase peptide synthesis. *RSC Advances* **5(126)**, 104417-104425 (2015).

[42] Caplan, M. R., Moore, P. N., Zhang, S., *et al.* Self-assembly of a β-sheet protein governed by relief of electrostatic repulsion relative to van der Waals attraction. *Biomacromolecules*, **1(4)**, 627-631 (2000).

[43] LeVine III, H. Quantification of β-sheet amyloid fibril structures with thioflavin T. In Methods in enzymology (Vol. 309, pp. 274-284). Academic Press, (1999).

[44] Hancock, R. D., Marsicano, F. Parametric correlation of formation constants in aqueous solution. 2. Ligands with large donor atoms. *Inorganic Chemistry* **19(9)**, 2709-2714 (1980).

[45] Lear, S., Cobb, S. L. Pep-Calc. com: a set of web utilities for the calculation of peptide and peptoid properties and automatic mass spectral peak assignment. *Journal of Computer-Aided Molecular Design* **30(3)**, 271-277 (2016).

[46] Dong, H., Snyder, J. F., *et al.* Cation-induced hydrogels of cellulose nanofibrils with tunable moduli. *Biomacromolecules* **14(9)**, 3338-3345 (2013).

[47] Stendahl, J. C., Stupp, S. I. Intermolecular forces in the self-assembly of peptide amphiphile nanofibers. *Advanced Functional Materials* **16(4)**, 499-508 (2006).

[48] Beniash, E., Hartgerink, J. D., Stupp, S. I. Self-assembling peptide amphiphile nanofiber matrices for cell entrapment. *Acta Biomaterialia* **1(4)**, 387-397 (2005).

[49] Singh, T. R. R., Laverty, G., Donnelly, R. Hydrogels: Design, Synthesis and Application in Drug Delivery and Regenerative Medicine. *CRC Press*, 292 (2018).

[50] Peh, E., Liedel, C., Taubert, A., Tauer, K. Composition inversion to form calcium carbonate mixtures. *CrystEngComm* **19(26)**, 3573-3583(2017).

[51] Roller, S., Röhr, C. "Strukturtypen-Datenbank: Rutil-Typ (C4-Typ)" Vorlesung Chemie der Metalle, Institut für Anorg. u. Analy. Chemie, Univ. Freiburg, AK Röhr, $http://ruby.chemie.uni-freiburg.de/Vorlesung/Strukturtypen/ab2_rutil.html$.

[52] Sieste, S., *et al.* Water-Dispersible Polydopamine-Coated Nanofibers for Stimulation of Neuronal Growth and Adhesion. *Advanced Healthcare Materials* (2018).

[53] XU, D., *et al.* Self-assembly of Filamentous Cell Penetrating Peptides for Gene Delivery. *Humana Press* **Peptide Self-Assembly** 271-281 (2018).

[54] AliExpress, "Präzision Bohrfutter Keyless". Retrieved from $https://de.aliexpress.com/$.

[55] Goldschmiedebedark Otto Simon e.K., "Biegsame Welle". Retrieved from $http://www.goldschmiedewerkzeug24.de/Welle-Kugellager$.

[56] Metabowerke GmbH, "FME 737 Oberfräse". Retrieved from $https://www.metabo.com/de/de/$.

6 Appendix

6.1 Zone Casting: Measured Data

Table 6.1: Table with the tested parameters during zone casting. First a variety of different values was tested before returning to temperatures and speeds that were found to be apropriate for the system. Samples which displayed a more homogeneous appearance are labelled with a check and resembled the coat displayed in Figure 3.22.

	syringe speed	substrate speed	solution temperature	substrate temperature	Evaluation
Run 1	50 μm/s	20 μm/s	RT	RT	
Run 2	50 μm/s	20 μm/s	50 ℃	50 ℃	
Run 3	50 μm/s	20 μm/s	60 ℃	70 ℃	
Run 4	50 μm/s	20 μm/s	70 ℃	100 ℃	
Run 5	70 μm/s	20 μm/s	40 ℃	40 ℃	
Run 6	70 μm/s	20 μm/s	50 ℃	50 ℃	
Run 7	70 μm/s	20 μm/s	70 ℃	70 ℃	
Run 8	70 μm/s	20 μm/s	70 ℃	100 ℃	
Run 9	20 μm/s	20 μm/s	40 ℃	40 ℃	
Run 10	20 μm/s	40 μm/s	60 ℃	50 ℃	
Run 11	20 μm/s	60 μm/s	60 ℃	50 ℃	
Run 12	20 μm/s	80 μm/s	60 ℃	50 ℃	
Run 13	20 μm/s	100 μm/s	60 ℃	50 ℃	
Run 14	25 μm/s	20 μm/s	50 ℃	70 ℃	✓
Run 15	25 μm/s	15 μm/s	50 ℃	70 ℃	✓
Run 16	20 μm/s	20 μm/s	50 ℃	70 ℃	✓
Run 17	20 μm/s	15 μm/s	50 ℃	70 ℃	✓
Run 18	20 μm/s	10 μm/s	50 ℃	70 ℃	✓
Run 19	20 μm/s	20 μm/s	50 ℃	80 ℃	✓
Run 20	20 μm/s	20 μm/s	50 ℃	90 ℃	
Run 21	20 μm/s	20 μm/s	50 ℃	100 ℃	
Run 22	15 μm/s	20 μm/s	50 ℃	70 ℃	✓
Run 23	15 μm/s	15 μm/s	50 ℃	70 ℃	✓
Run 24	15 μm/s	10 μm/s	50 ℃	70 ℃	
Run 25	15 μm/s	7 μm/s	50 ℃	70 ℃	
Run 26	15 μm/s	5 μm/s	50 ℃	70 ℃	
Run 27	15 μm/s	10 μm/s	50 ℃	70 ℃	
Run 28	15 μm/s	10 μm/s	50 ℃	60 ℃	
Run 29	15 μm/s	10 μm/s	50 ℃	80 ℃	
Run 30	15 μm/s	10 μm/s	50 ℃	100 ℃	